NTNU – Trondheim
Norwegian University of
Science and Technology

Hydrological Modelling of the Ilabekken Catchment, and Flood Simulations of Ilabekken using HEC-HMS and HEC-RAS

Lise Østlid Bagstevold

Civil and Environmental Engineering
Submission date: June 2015
Supervisor: Tone Merete Muthanna, IVM

Norwegian University of Science and Technology
Department of Hydraulic and Environmental Engineering

Abstract

As the global climate is changing, the local climate in Trøndelag is expected to be wetter and more extreme in the future. Flooding and erosion are huge challenges in Norway, leading to severe damages each year which lead to large costs for the society. As a result, the society demands a greater focus on the climate change impacts.

The aim of this thesis is to investigate how the climate change will impact the risk of erosion and flooding in Ilabekken, an urban stream in Trondheim. This will be done by creating a hydrological model of the catchment upstream of Ilabekken, and a river model of the upper part of Ilabekken, using the software HEC-HMS and HEC-RAS. The thesis includes a calibration of the HEC-HMS model by using observation data from Kobberdammen, located in the upper part of the catchment. To be able to establish the HEC-RAS model, surveying the river geometry has been conducted. The stability in the stream can be evaluated by investigating the hydraulics in the stream. Computation of the stable stone sizes in parts of the stream exposed to erosion has been done using the Shields equation and the HEC-11 method.

The 200 year flood event is computed to be 17.14 m^3/s. This magnitude is based on a 6 hours synthetic storm event computed by statistical precipitation data from Voll observation site. The simulation shows that Theisendammen will have a damped effect on the runoff. Since there are three larges lakes in the catchment, these will likely have a reducing effect and contribute to a delay of the runoff. During a 200 year flood event it will likely be flooding in the lowest part of the modelled reach. The simulations shows that increasing flood magnitudes could lead to a flow pattern producing hydraulic jumps at several places along the stream which could possibly cause erosion.

The main trend in the computations of D_{50} indicate that increasing runoff will induce larger stable stone sizes, however this is not the case in all part of the stream. In shallow areas the size of D_{50} will decrease with increasing runoff due to higher water depths and decreasing velocity. The computations of stable stone size show a great difference between the methods. The results shows that the HEC-11 method is very sensitive when the angle of the side slope approach the angle of repose. This method should be used carefully when estimating stable stone sizes in steep side slopes.

Transport of sediments can lead to sedimentation in the lower part of the stream where the velocity decreases due to more shallow areas. It has already been observed in the lower part of the stream. A consequence is poorer biological diversity in the area, due to accumulation of sediments.

Sammendrag

Klimaendringene vil fører til økning i både temperatur og nedbør i Trøndelag. Mye tyder på at det fremtidige klimaet vil bli mer vått og ekstremt, der både nedbørsvolumet og intensiteten vil øke. Hvert år fører flomrelaterte skader til store kostnader for samfunnet. Som et resultat av dette er det større fokus på å redusere riskoene for flom og erosjon.

Bakgrunnen for denne masteroppgaven er å undersøke hvordan klimaendringene vil påvirke faren for flom og erosjon i Ilabekken, som er en urban bekk i Trondheim. Oppgaven består av å lage en hydrologisk modell av nedslagsfeltet over Ilabekken ved bruk av programmet HEC-HMS, og deretter lage en HEC-RAS modell av øvre del av bekken. Den hydrologiske modellen gjør det mulig å undersøke responsen i nedbørsfeltet og estimere størrelsen på 200 års flommen. HEC-HMS modellen har blitt kalibrert mot observerte vannføringer i Kobberdammen som ligger i øvre del av nedslagsfeltet. HEC-RAS modellen gjør det mulig å undersøke faren for flom og erosjon i Ilabekken. For å lage HEC-RAS modellen har det vært nødvendig å gjøre oppmålinger av geometrien til bekken. Det har blitt gjennomført en evaluering av stabile steinstørrelser i erosjonsutsatte tverrsnitt ved hjelp av Shields formel og HEC-11 metoden.

Resultater fra simuleringene i HEC-HMS viser at den simulerte 200 års flommen er på 17.14 m^3/s. Denne størrelsen er basert på syntetisk nedbør beregnet fra statistiske nedbørsdata fra Voll målestasjon, med en varighet på 6 timer. Simuleringen viser at det vil være en flom dempning i dammene i nedslagsfeltet. Simuleringene i HEC-RAS viser at økning i flomstørrelsen vil føre til et strømningsmønster der det oppstår vannstandssprang flere steder i bekken slik at erosjon kan oppstå på disse stedene. Hovedtrenden i beregningene av D_{50} viser at økende flomstørrelser gir økende stabile steinstørrelser, men dette er ikke tilfellet i alle deler av bekken. På slakere partier vil D_{50} bli redusert ved økning i vannføringen på grunn av høyere vannstand og en reduksjon av hastigheten. Resultatene viser at de to metodene gir store variasjoner i flere av tverrsnittene. HEC-11 metoden er vist å være svært sensitiv til bratte sidehelninger.

Sedimenttransport fra øvre del kan bidra til nedslamming i slakere partier i den nedre delen av Ilabekken. Dette har allerede blitt observert. En konsekvens til dette er en reduksjon i det biologisk mangfold i området.

Preface

This thesis mark the end of the Master Degree in Hydraulic and Environmental Engineering at the Norwegian University of Science and Technology (NTNU). The thesis has been accomplished during the spring 2015.

The thesis includes the establishment of a hydrological model using HEC-HMS and a flood simulation model using HEC-RAS. The HEC-RAS model requires field work surveying cross sections of the river. Parts of the survey were conducted during previously work in the fall of 2014, and the remaining field work has been perform during this thesis.

The thesis includes several different topics, which have made the work various and interesting. It has been an educational and challenging semester, and I have gained lots of experience which will be useful in further work. I would like to thank my supervisor Tone M. Muthanna, Associate Professor at the Department of Hydraulic and Environmental Engineering for help and guidance during the semester. I would also like to thank Professor Knut Alfredsen, which has provided assistance in the use of the equipments needed in the field work. Additionally, Petter Reinemo at Asplan Viak has been helpful in the establishment of the HEC-RAS model. Erlend Nygård, Olav Nilssen and Terje Nøst at the municipality of Trondheim have been helpful providing information of the studied area.

Lastly, I would like to thank Espen Bengtson for help and support during the writing process.

Lise Østlid Bagstevold
Trondheim, June 10, 2015

Contents

List of Figures

List of Tables

Chapter 1

Introduction

The global climate is changing leading to increase in the average temperature and a more unequal distribution of water globally [IPCC, 2014]. In Norway the average temperature is increasing and there is an increase in both precipitation volume and intensity. The climate in Norway has become wetter and more extreme, and research shows that this will increase in the future [Hanssen-Bauer et al., 2009]. Flooding and erosion are huge challenges in Norway leading to severe damage each year. Numbers from Norwegian Natural Perils Pool show that the compensation of natural damage for 2014 is more than 650 million NOK [Finans Norge, 2015]. More than 60 % of the compensation is from damages after flooding. As a result, the society demands a greater focus on the climate change impacts. It is important to investigate the interaction between hazards, triggered by an event or trend related to climate change, the vulnerability and exposure of people, assets or ecosystems at risk [IPCC, 2014].

The aim of this thesis is to investigate how the climate change will impact the risk of erosion and flooding in Ilabekken, an urban stream in Trondheim. This will be done by creating a hydrological simulation model of the catchment upstream of Ilabekken, and a river analysis model by using the software HEC-HMS and HEC-RAS, respectively. Simulation of the hydrological response in the catchment makes it possible to evaluate how the processes in the catchment will impact the runoff to Ilabekken. HEC-RAS allows for simulations of different flow regimes, making it achievable to study the changes in the flow pattern which can lead to more erosion and flooding. The stability in the stream can then be evaluated, by investigating the hydraulics in the stream.

The lower part of Ilabekken went through a reopening process in 2006 where the city of Trondheim used a lot of resources to create a stream with biological diversity, high hydraulic capacity and with nice esthetically surroundings. To

maintain the condition of this area, it is of interest to investigate how the stream will respond to a changed flow pattern due to climate change and what kind of consequences this can result in. It is beneficial for the society that the risks caused by erosion and flooding are examined, making it possible to protect and try to prevent damages in the future. The thesis will estimate the risk of erosion and flooding in the upper part of Ilabekken, and evaluate the necessity of erosion protection measures. Often can efforts upstream in a river systems prevent problems with erosion, sedimentation and flooding downstream in the river.

1.1 Study Area

Ilabekken is an urban stream located in Trondheim in the county of Sør-Trøndelag, Norway. The stream is known for high flows, and historical observations show that the area has been exposed for large flood events. The outlet from the stream head water, Theisendammen is a broad crested overflow dam. From here the stream flows roughly 2 km before reaching the ocean at Ilsvika. The catchment area of Ilabekken is shown in figure 1.1. The area of the whole catchment is roughly 9.4 km^2, with an elevation difference ranging from 0 to 546 m.a.s.l. The upper part of the catchment contains mostly forest and marches. The forest area is mainly coniferous, but there is also parts with broad-leaved trees. There are three lakes located in the catchment, Kobberdammen, Baklidammen and Theisendammen. These lakes were originally used for water supply and industry, but today they are only used for recreational purposes. The dams are unregulated, which means that the water will flow over the spillway when the storage capacity is exceeded. From Baklidammen the water flows over an ogee weir, and at the outlet of Kobberdammen it is a V-notch weir. The part of the catchment downstream from Theisendammen is more impervious with urban areas of buildings and roads.

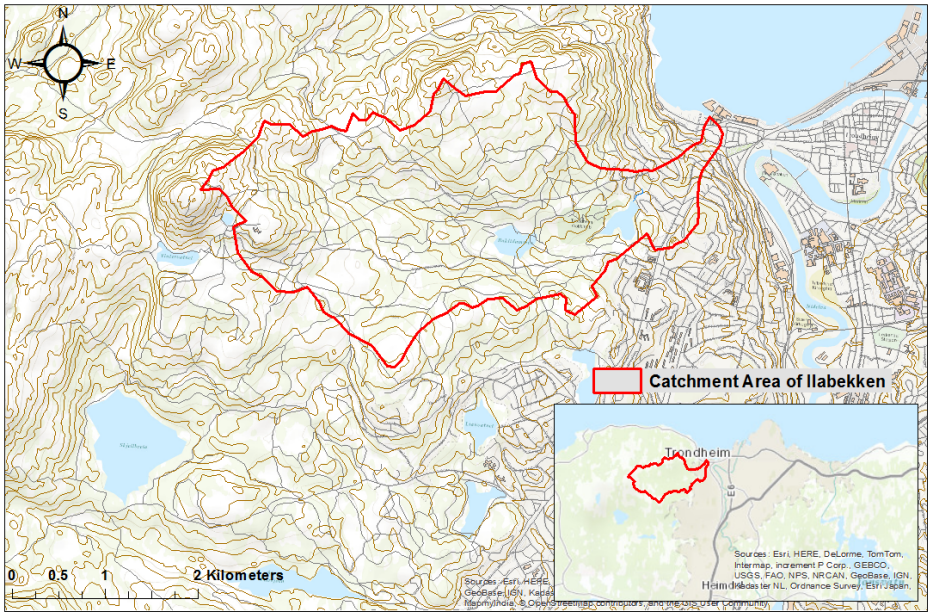

Figure 1.1: Catchment area of Ilabekken

Before the reopening of the lower part in 2006, the stream ran through pipes, and the water quality was generally poor due to spill of sewerage from buildings. The reopening process included ponds, fish ladders and reconstruction of the sewer system. These efforts have lead to an improved water quality, increased biological diversity and made it possible for fish spawning [Bergan, 2010]. The area has also become an important place for recreation. There is a low flow valve regulating and ensuring a minimum flow of 60-80 l/s throughout the year from Theisendammen. To obtain a minimum flow in the stream is important for securing living conditions for anadromous fish, such as sea-trout. In the last years it has been an increasing tendency of sedimentation in the reopened part of Ilabekken [Nøst, 2014].

In this thesis the part of the stream which flows 420 m downstream from Theisendammen is modelled in HEC-RAS. This part contains mainly natural stream segments with riparian vegetation. From the outlet of Theisendammen the water drops 10 m and flows under a bridge. This part of the stream contains bare rocks and has at the right side an existing erosion protection wall. Around 50 m downstream from the outlet of Theisendammen a V-notch weir is located. This weir is not operative, however it will effect the flow in the stream. Further

down the water flows through a steep area before reaching a more shallow part. At the end of the modelled reach, the water will flow through a 18 m long culvert under Reservedammen. Further down, the stream flows down Iladalen which is a valley with steep side slopes and lots of vegetation along the stream. The reopened part is the last 700 m of the stream is the reopening part containing more urban elements towards the stream end at Ilsvika.

Chapter 2

Hydrology

2.1 A Changing Climate

The global climate is driven by the earths energy balance which is the difference between total incoming and outgoing energy. Changes in the earths energy budget is mainly affected by the variations in solar radiation, the amount of greenhouse gases in the atmosphere, and changes in the reflectivity of the atmosphere and earth surface. The global climate system is in constant change with natural variations. However, over the last decades the observations shows that the global climate is in a clear change. The latest report from the Intergovernmental Panel on Climate Change (IPCC) concludes that the human influence on the climate system is clear, and recent man-made emissions of greenhouse gases are the highest in history [IPCC, 2014]. The level of atmospheric concentrations of carbon dioxide, methane and nitrous oxide has not been higher in at least 800,000 years. The emissions of the greenhouse gases are very likely to have been the main cause of the observed warming since the mid-20th century. The consequences are an increase of the ocean temperature and a reduction in snow and ice covers, leading to a higher global mean sea level. These observations are shown graphical in figure 2.1. This figure shows a strong trend of an increasing global average surface temperature, sea level and a decrease in the snow cover in the Northern Hemisphere. All differences are relative to corresponding averages for the period 1961-1990.

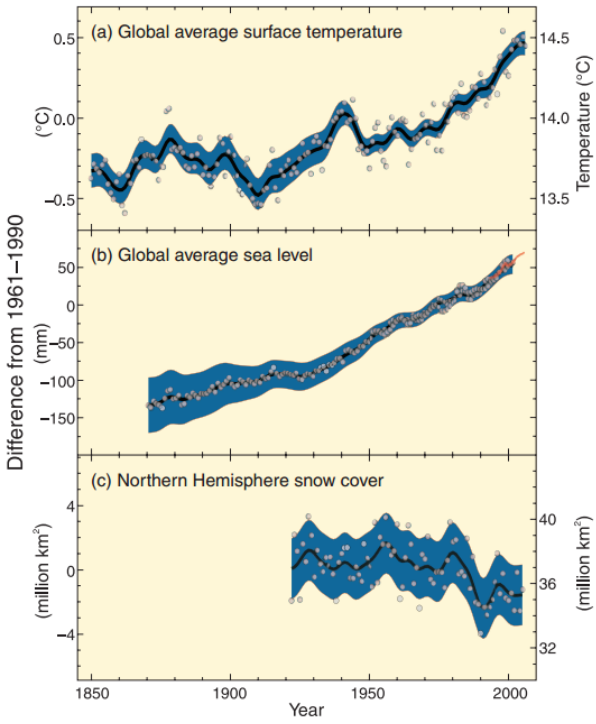

Figure 2.1: Observed changes in the average surface temperature, sea level and the Northern Hemisphere snow cover, adapted from Barker et al. [2007]

Knowledge on how the climate change will impact each region of Norway is presented by Hanssen-Bauer et al. [2009] in the report *Klima i Norge 2100*. The aim of this report was to develop an evaluation of the societies vulnerability and need for adaption as a result of the changing climate. The basis of this knowledge is mainly based on the IPCC report from 2007 which, at the time was the latest report. Since the Norwegian report was developed in 2009, the global climate models and emission scenarios have been modified. The newest knowledge concerning the science of climate change are found in the latest report from IPCC published in 2014.

2.1.1 Downscaling Climate Projections

Since emissions of greenhouse gases have great impact on the climate, the future climate will depend on the development of these emissions. To be able to pre-

dict how the climate will be in the future, emission scenarios can be used which includes a range of different pathways. The emissions of man-made greenhouse gases are driven by several factors, mainly by economic and population growth, lifestyle, changes in energy use and technology, land-use patterns and climate policy [IPCC, 2014]. The scenarios are alternative images of how the future might unfold. These are appropriate tools to analyse how the driving factors may influence future emission outcomes, and to assess the associated uncertainties [Nakicenovic and Swart, 2000]. The possibility that any single emission path will occur is highly uncertain, however these scenarios give a hint on how the future climate will be. The emission scenarios are based on global climate models. These models describe a physical reality with background in mathematical approximation and statistical analysis. The previous IPCC assessments are based on the Special Report on Emission Scenarios presented by Nakicenovic and Swart [2000] which describe several different scenarios. In the latest report from IPCC the previous emission scenarios are modified to cover an wider range as they also represent scenarios including climate policy.

The global climate models have generally poor spatial dimension, typically 200 x 200 km [Hanssen-Bauer et al., 2009]. To get a better spatial resolution and improve the regional climate projections it is necessary to downscale the results from the global climate models. This can be done by using several methods, divided into dynamical and statistical methods. Dynamic methods are based on the same physical equations which are used in the global climate models. Statistical methods are based on historical observations which are used to identify and quantify statistical connections between the global climate and the local. The statistical method gives a more local adaptation than the dynamical methods, while the dynamical is more adapted to the physical system since physical equations are the basis of the method. The results in the Norwegian report are based on both dynamical and statistical methods, including 22 different climate projections downscaled with dynamical methods, and 50 climate projections calculated from statical methods. In this report the results are split into three scenarios, low, medium and high. These scenarios are based on the average of the projections from the dynamical and statical methods. Low is 10 % of the average of the projections, medium is the average value and high is defined as the value that exceeds 90 percent of the projections. The results in the report which are applicable for Trøndelag are presented in table 2.1 and table 2.2. These results show the variation throughout the year regarding temperature change and the precipitation change for the period between 2071 and 2100. Table 2.2 shows the change in numbers of days with lots of precipitation, and the change in the amount of precipitation at these days. Days with lots of precipitation are defined as days with precipitation amounts which in the reference period 1961-1990 was exceeded in 0.5 % of the total days.

	Temperature change (°C at 2071-2100 relative 1961-1990)			Precipitation change (% at 2071-2100 relative 1961-1990)		
Scenario	Low	Medium	High	Low	Medium	High
Annual average	2.2	3.2	4.4	1.1	22.5	51.8
Winter	2.6	4.1	5.8	-11.6	18.6	36.5
Spring	2.1	3.3	4.6	5.7	22.6	57.4
Summer	1.0	1.9	3.0	8.0	21.1	36.1
Autumn	2.3	3.4	4.8	0.9	28.3	60.8

Table 2.1: Change in temperature and precipitation for Trøndelag at 2071-2100 relative to 1961-1990

	Change in number of days with lots of precipitation (% at 2071-2100 relative to 1961-1990)			Change in the amount of precipitation at days with lots of precipitation (% at 2071-2100 relative to 1961-1990)		
Scenarios	Low	Medium	High	Low	Medium	High
Annual average	9.1	68.6	183.7	13.9	13.9	32.8
Winter	-43.2	86.5	172.9	13.2	13.2	33.5
Spring	7.5	65.1	184.6	11.1	11.1	33
Summer	17	90.1	158.1	19.4	19.4	36.6
Autumn	5.7	92.7	310.1	13.9	13.9	38.8

Table 2.2: Change in number of days with lots of precipitation for Trøndelag at 2071-2100 relative to 1961-1990

2.2 Hydrological Processes

How the water will be distributed in the hydrological system is of importance to understand the hydrological processes in a catchment. The distribution of the fallen precipitation will be the sum of water stored in the catchment, the amount of the precipitation which will go back to the atmosphere through evapotransration, and the runoff from the catchment. The relation between these processes is shown in the general water balance in equation 2.1.

$$P = Q + ET + \Delta S \tag{2.1}$$

Where P is precipitation, Q is discharge including the surface runoff and base flow, ET is the evapotranspiration and ΔS is the change in water storage.

In natural systems some of the fallen precipitation will be transported back to the atmosphere through evaporation and transpiration through plants. The infiltration of water represent the movement beneath the surface, and will depends on the type of soils in the catchment. How great the runoff will be depends on several factors. The distribution of vegetation and land-use cover in the catchment will have an effect on the runoff, as catchments with lots of vegetation and sediments have more damped runoff that catchments with bare rocks or urban

areas with impervious surfaces. The presence of water bodies such as lakes and marshes in the catchment will affect the response of the runoff. For instance, lakes located near the outlet of the catchment will have a higher effect on flood reduction than lakes near the drainage divide. The initial state of the catchment will influence the magnitude of the runoff. If the catchment is dry after a long period of warm weather, the precipitation will effect the runoff less as the water will first be infiltrated in the catchment. If the same amount of precipitation falls when the catchment is already soaked, the runoff will be higher. Floods can be a result of snow melt, snow melt in combination with precipitation, long-lasting precipitation or precipitation events with high intensity.

Of the different part of the water cycle, the evapotranspiration is the hardest parameter to estimate. While precipitation and runoff can be quantified, it is more difficult to measure the evapotranspitration directly. This parameter depends on several factors like soil, air and water temperature, solar radiation, wind and type of vegetation [Gilli et al., 2012].

2.3 Hydrological Data

To be able to estimate how the climate in Trondheim affects the runoff, historical observation data from the local area can be used. The official meteorological observation station in Trondheim is located at Voll, at 127 m.a.s.l and roughly 5 km from Theisendammen. The station was established in 1923, and has long data series with good quality. Time series of precipitation and temperature observated at Voll, can be downloaded from the web portal *Eklima* which gives free access to the climate database operated by Norwegian Meteorological Institute.

One way to estimate the magnitude of a flood with a certain return period is to use a depth-duration-frequency (DDF) analysis. This is an estimation of rainfall depths with given return periods with various storm durations at a given precipitation-gauge location. The precipitation depths from Voll observation site are shown in table 2.3. The likelihood of a flood event occurring is usually expressed in terms of its predicted return frequency. For instance, a 200 year flood has a 0.5 % probability of being equaled or exceeded on average each year.

	Precipitation depth [mm] at varying storm duration							
Return period	15 min	30 min	60 min	90 min	120 min	180 min	360 min	720 min
100	12.3	14.9	22.1	28.4	37.2	44.7	60.3	77.8
200	13.2	15.9	23.9	30.9	40.9	49.0	65.9	84.7

Table 2.3: Depth-duration-frequency

At the outlet of Kobberdammen there is a measurement station operated by the Norwegian Water Resources and Energy Directorate (NVE). The station is

located at 288 m.a.s.l, and has a catchment area of 0.82 km^2. The observed discharge for Kobberdammen are given for each hour. The time series used are downloaded from NVE's database Hydra II. The outlet is a sharp-crested V-notch weir. Discharge through the weir can determined by measuring the water level above the point of the V-notch, and relating that elevation to discharge. Equation 2.2 presented the discharge through a V-notch weir [Ødegaard, 2012].

$$Q = \frac{8}{15} C tan \frac{\alpha}{2} \sqrt{2g} H^{5/2} \tag{2.2}$$

Where α is the angle of the V [°], C is the weir coefficient (0.585 for $\alpha = 90°$) and H is the difference between the water level upstream the weir and the bottom of the angle point [m].

Voll observation site does not include observation of evaporation. It will be necessary to compute it from the temperature data. Potential evaporation is computed using the Thornthwaite's equation which is based on the average monthly temperature which is presented in equation 2.3 [Gilli et al., 2012].

$$PET = 16(10\frac{t}{I})^a \tag{2.3}$$

$$I = \sum (\frac{t}{5})^{1.514} \tag{2.4}$$

$$a = 6.75 * 10^{-7} * I^3 - 7.71 * 10^{-5} * I^3 + 1.79 * 10^{-2} * I + 0.4923 \tag{2.5}$$

Where PET is monthly average evaporation [mm], t is average monthly temperature [°C] and I is a heat index for a given year.

2.3.1 Local Climate Factors

Predicting the magnitude of flood events, one must include expected changes in flood magnitude due to climate change. In the NVE report 5-2011 local guidelines of climate change impacts throughout Norway are presented. The recommendation for Trøndelag is to increase the flood magnitude with 20 % for calculation of changes in the 200 year, 500 year and 1000 year flood until 2100 for catchment areas smaller than 100 km^2 [Lawrence and Hisdal, 2011]. All catchments under 100 km^2 are projected to have an 20 % increase in the flood magnitude under a future climate. This is in response to show that short-term extreme precipitation will increase throughout the country, and that smaller catchments are most vulnerable to this increase. The basis for the guidelines are simulations derived from the large-scale global climate models and detailed hydrological modelling of unregulated catchment distributed throughout Norway.

Chapter 3

Flow in Natural Streams

3.1 Open Channel Hydraulics

Flow in open channels can be classified from three reference points, which are:

- Subcritical or supercritical flow
- Steady or unsteady flow
- Uniform or nonuniform flow

The total energy in the flow in a section with reference to a datum line is the difference between the elevation Z, the water depth Y, and the velocity head $V^2/2g$. In open channel flow the water level is equal to hydraulic grade line, while the flow energy is represented to as the energy grade line. Loss of energy results when water flow from one section to the next, which is represented by the energy head loss h_f. These relations are presented in the Energy equation 3.1 [Brunner, 2010].

$$Z_2 + Y_2 + \frac{V_2^2}{2g} = Z_1 + Y_1 + \frac{V_1^2}{2g} + h_f \tag{3.1}$$

The Froude number is the ratio of inertial force to gravity forces presented in the equation 3.2. This relation states if the flow is either subcritical, critical or supercritical.

$$Fr = \frac{V}{\sqrt{gD}} \tag{3.2}$$

Where Fr is the Froude number and D is a characteristic depth [m]. The flow is critical when the Fr equals 1, subcritical when the Fr is less than 1 and supercritical when the Fr is greater than 1 [Crowe et al., 2010]. The transition from subcritical to supercritical and vice versa can occur at several instances, such as significant changes in the channel slope, drop structures, weirs, or other flow obstructions. The flow in natural streams are often subcritical, however the flow in steep falls or over spillways are supercritical. The effect of the viscosity of water relative to inertia can be represented by Reynolds number shown in equation 3.3.

$$Re = \frac{VR_h}{\upsilon} \tag{3.3}$$

Where υ is the kinematic viscosity of water $[mm^2/s]$ and R_h is the hydraulic radius. If the Re is less than 500 in open channels, the flow is laminar, if Re is greater than 750 the flow will be turbulent [Crowe et al., 2010]. A brief analysis of this criterion shows that the flow in channels usually is turbulent unless the velocity and/or the depth is very small.

As stated earlier in the section, the flow in open channels is described as either uniform or nonuniform. For uniform flow the velocity is constant along the streamline, which means that the cross section and depth do not change along the length of the channel. The discharge in a open channel is often computed by the Manning formula presented in equation 3.4 [Crowe et al., 2010]. This formula is applicable for uniform flow for open channels. The depth for uniform flow conditions is referred to as normal depth.

$$Q = \frac{1}{n} A R_h^{2/3} \sqrt{S} \tag{3.4}$$

Where n is the roughness coefficient, A is the cross-sectional area of flow, and S is the channel slope. S is in fact the slope of the hydraulic grade line, since the depth is constant, the slope of the hydraulic grade line will be the same as the slope of the channel bed.

In a nonuniform flow the velocity changes along the channel due to changes in the channel depth. The flow in natural streams are often nonuniform due to difference in depth and irregular cross sections along the streamline. In a steady nonuniform flow the velocity and depth change over the distance, but not over time. A nonuniform flow can either be referred to as a rapidly varied flow or as a gradually varied flow, depending on whether the change of velocity and depth occurs over a short or long distance of the channel. In rapidly varied flow the channel resistance is negligible. An example of a rapidly varied flow is a hydraulic jump which occurs when the flow along the channel changes from supercritical to subcritical. Hydraulic jumps are often created by weirs or steep falls. A hydraulic jump result in a sudden increase in the depth, turbulent flow and a large energy loss.

The most complex open channel flow is unsteady nonuniform flow. In an unsteady nonuniform flow every condition of the flow can change with time along the distance of the stream.

3.2 Erosion Processes

Erosion, transport and deposition of sediments are more or less continuous processes in all natural streams. Erosion occurs when more mass are removed than accumulated. There are mainly two processes which contribute together; mass movement in side slopes and lateral- and bed erosion [Jenssen and Tesaker, 2009]. The greatest erosion occurs in lateral turns, and where the water has the highest velocity against the river bank. The deposition of sediments will often be greatest at the inner curves of the stream, and at shallow parts with low velocity.

In channel bends the flow conditions are complicated by the distortion of flow patterns. In long, relatively straight channels, the flow conditions are uniform, and symmetrical about the center line of the channel. In channel bends however, the centrifugal forces and secondary currents produced, lead to non-uniform and non-symmetrical flow conditions [Brown and Clyde, 1989]. Figure 3.1 shows where to expect the greatest erosion in bends. As the figure indicates the greatest erosion will occur around two channel widths downstream from the point where the center line crosses the river bank [Fergus et al., 2010].

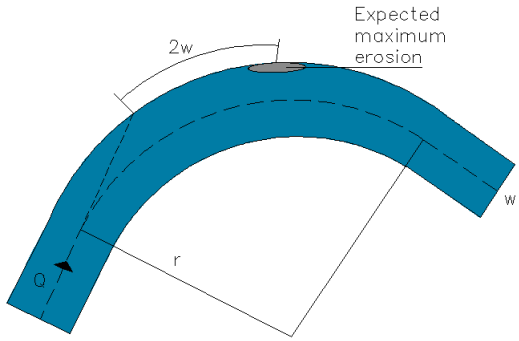

Figure 3.1: Straining point of erosion in channel bends

The vertical flow distribution is roughly the same over the whole width when the water flows over a flat and wide channel bed. In channels with narrow and irregular width the sides will influence the flow distribution, giving the highest

velocity in the center of the main channel [Jenssen and Tesaker, 2009]. To maintain continuity the water will flow across the section of the stream, developing a lateral flow pattern. Lateral flows can lead to local erosion or deposition due to uneven distribution of the shear stress. The transition between subcritical and supercritical flow implies increasing velocity and shear stress which also increase the risk of local erosion. Erosion in stream bed can be caused be a hydraulic jump described in section 3.1 as lots of energy are released.

In order to erosion could occur, energy must be used. Stream power is a measure of the energy transfer of the water flow. Stream power can be used as an indicator of erosional forces acting on the channel bed and the overbanks. The stream power is defined as presented in equation 3.5 [Berenbrock et al., 2007]. As the equation shows, the stream power is a product of shear stress and velocity.

$$\Omega = \tau V = (\gamma DS)\, V \tag{3.5}$$

Where Ω is the stream power [N/ms], τ is the shear stress $[N/m^2]$, γ is the specific weight of water $[N/m^3]$.

Particle erosion is the most common type of erosion process, which is normally caused by the water flow, however ice and flotsam can also contribute to particle erosion [Jenssen and Tesaker, 2009]. Eroded particles which accumulate at new places in the stream can lead to more concentrated flow and more erosion. It is several relations which can contribute to particle erosion, such as too steep side slopes, the stone diameter is to small to resist the water flow or erosion which undermines the slope of the river bank. The greatest erosion and sediment transport will normally occur during a flooding. In what degree depends on type of sediments at the location, the flow pattern and the forces against the exposed area. Changes in the flow pattern can lead to erosion occurring at new part of the stream.

3.3 Channel Stability

The channel stability depends on the ratio of the average tractive force exerted by the water and the critical shear stress of the river material. If the critical shear stress of the material is greater than the tractive stress induced by the flow, the material is considered stable. Evaluation of channel stabilization is essential to the design of protection measurement in a stream. The identification of the potential for channel bank erosion, and the following need for channel stabilization, is best accomplished through observation [Brown and Clyde, 1989]. However, analytic methods are available for the evaluation of channel stability. Hydraulic relationships for evaluating channel stability are based on an analysis of site materials, and the ability of these materials to resist the erosive forces

produced by a given design discharge. The stability of a particular stone is a function of its size, expressed either in terms of its weight or equivalent diameter. In design of protection measurements in a stream the most common way to grade stones is according to diameter. It is normal to choose D_{50} as the default stone size [Jenssen and Tesaker, 2009]. D_{50} is the median stone diameter, which indicates the size where 50 % of the total stone material is smaller, by weight.

The stable stone size, D_{50}, can be estimated by both the shear stress or the velocity. Two methods used for estimating the stable stone size are describe in the next sections. These methods will only provide a point of reference for evaluating channel stability against particle erosion. Particle erosion is only one of several erosion mechanisms which can cause channel instability.

3.3.1 Shields Equation

A common method used for estimating stable stone size base on shear stress is the Shields equation, presented in equation 3.6 [Jenssen and Tesaker, 2009]. The relation is estimated by experiments, and the method includes the effect of viscosity, expressed by the Reynolds number. The viscosity of the water make a tight layer of laminar flow at the bottom, influencing the stability.

$$C = \frac{\tau}{0.05g(\rho_s - \rho_w)D} \tag{3.6}$$

Where C is a dimensionless shear stress, ρ_s is the density of the stone, ρ_w is the density of water and D is the particle diameter. Equation 3.6 can be expressed in terms of the stable diameter of the stone. Then C equals to 0.05 which is refereed to as the stability line between the C and Reynolds number.

When computing the D_{50} in lateral turns with Shields equation, a correction factor must be included by estimate the ration between the curve radius and the channel width, expressed as the R/W ratio. There is also important to include the effect of the side slope in the cross section. These correction factors can be found in literature. For the Shields equation it is normal to include a stability factor in addition to these factors, since the stability line of C=0.05 could vary [Jenssen and Tesaker, 2009].

3.3.2 HEC-11 Method

An other method used for estimating stable stone sizes is the HEC-11 method, presented in equation 3.7. This method uses flow velocity and depth as its controlling parameters. The methods is based on Shields equation, in addition to

include experiments regarding the stability factor.

$$D_{50} = 0.00594 C_{sg} C_{sf} \frac{V_{ch}^3}{\sqrt{y_{ch}}[1 - \frac{sin^2\theta}{sin^2\varphi}]^{0.75}} \tag{3.7}$$

$$C_{sg} = \frac{2.12}{(s-1)^{1.5}} \tag{3.8}$$

$$C_{sf} = (\frac{SF}{1.2})^{1.5} \tag{3.9}$$

Where θ is the bank angle with the horizontal [degree], φ is the material angle of repose [degree], SF is stability factor [-], s is the specific density of the stone $[g/cm^3]$, C_{sg} is correction factor for s different from 2.65 [-] and $C_{sf}$is correction factor for SF different from 1.2. The angle of repose is the angle of slope formed by particulate material under the critical equilibrium condition of incipient sliding [Brown and Clyde, 1989].

The stability factor is the ratio between critical shear stress for the protection and the average shear stress between the river bed and flow. The stability factor depends on the flow regime in the observed part of the stream. If the stream is straight or has gentle curves (R/W $>$ 30), the stability factor is between 1.0 - 1.2. If the stream has curves with short radius (R/W $<$ 10) the factor is between 1.6 - 2.0 [Jenssen and Tesaker, 2009]. A high stability factor indicates a significant uncertainty in design parameters. The term in the square brackets considers the reducing of the stability when the stone protection is placed in a side slope.

Chapter 4

Modelling Approach

To be able to investigate how the future climate will affect the runoff in Ilabekken it is necessary to model the hydrological response in the catchment and how the runoff will flow in the stream. To achieve this, the software HEC-HMS and HEC-RAS have been used, respectively a hydrological modelling system and a river analysis system. Both programs are developed by US Army Corps of Engineers at the Hydrologic Engineering Center (HEC). Outflow curves from the HEC-HMS simulation are stored in HEC-DSS (Data Storage System) which can be imported to the HEC-RAS model.

4.1 Hydrological Modelling in HEC-HMS

HEC-HMS is designed to simulate hydrological processes in dendritic catchment systems. The program includes several models which can be used to perform different simulations. HEC-HMS includes primarily lumped models which means that there is no spatial variation in the model processes and characteristics. The program contains both empirical and conceptual models. A conceptual model is built by knowledge of the actual processes that influence the input, while an empirical model is built up by observations of the input and output, without trying to explicitly represent the transformation process. All the models in HEC-HMS are deterministic which means that all the input data and processes are free of random variation thus the model will always yield the same result from a set initial data [Feldman, 2000].

The aim of the simulations are to describe how the catchment will respond to the fallen precipitation to produce runoff. The model will represent the catchment behavior and simulate the runoff process. There are numerous methods available for the estimation of each process, HEC-HMS uses separate models for each

component of the runoff process. The selected methods are described below.

Runoff-Volume Model

The selected runoff-volume model (loss method) is the *initial and constant method*. The initial loss is equivalent to the amount of precipitation that will infiltrate before runoff begins. The constant loss rate is determined by the rate of infiltration that will occur after the initial loss is satisfied [Bulcock and Jewitt, 2010]. The method includes impervious surfaces as a percentage input of the total catchment area. In the catchment studied there is no considerable parts of impervious surfaces as most of the area contains forest and marches. This method is chosen, as there are limited soil data available for the catchment studying.

Direct Runoff Model

The transform method performs the actual surface runoff calculations within a subcatchment. The selected transform method is the *Clark unit hydrograph* which is a synthetic unit hydrograph method. This method does not require the user to develop a unit hydrograph through analysis of past observations. Instead the program uses a time versus area curve which develop a translation hydrograph from a storm event. The resulting hydrograph is routed through a linear reservoir which includes the effect of attenuation of storage across the subcatchment. This method requires input the time of concentration and a storage coefficient. Time of concentration defines the maximum travel time in each subcatchments while the storage coefficient account for storage effects in the linear reservoir [Bulcock and Jewitt, 2010].

Canopy Storage

The canopy method in the program represents the presence of vegetation in the catchment. Some precipitation will intercept in the plants reducing the amount of precipitation available for surface runoff. The selected method is the *simple canopy method*. In the simple canopy method all the precipitation are intercepted until the canopy capacity is exceeded. The input parameters are the initial canopy storage and the maximum storage capacity.

Surface Storage

The surface method includes the water accumulated at the surface as depressional storage from the net precipitation when the infiltration capacity is exceeded. When the amount of precipitation rate exceeds the infiltration capacity and the surface storage is filled, the surface runoff will begin. The maximum amount of water that can be stored on the surface before the surface runoff begin is

determined by the maximum surface storage. This parameter is a part of the selected *simple surface method*. In addition to the maximum surface storage, the initial storage must be specified.

Base flow Model

The selected base flow model is the *constant monthly base flow*. This method is primary intended for continuous simulations where the base flow is approximated by a constant flow for each month. In the simulation it is assumed the same base flow for each month throughout the year.

Routing Model

The selected routing method is the *lag route method* where the outflow is delayed by a user-specified lag time.
The computations are proceed from the upstream elements in a downstream direction. The program has the ability to represent a basin model with individual hydrological elements where the catchment is divided into several elements. The lakes in the catchment are included in the model as reservoir elements. The reservoir element in HEC-HMS can have several inflows and one computed outflow. In the reservoir element the water surface is assumed to be level. Several methods can be used to describe storage properties in a reservoir. While the reservoir element represents natural lakes behind dams, the actual storage simulation is calculated by routing methods within the reservoirs [Bulcock and Jewitt, 2010]. One of the routing methods is the outflow structures which can design the outflow from reservoirs with uncontrolled outflow structures. An other routing method is the outflow curve which represent the outflow from a reservoir with a known relationship between the storage and the discharge.

There are two different ways to describe the storage in the outflow structures method, either by the relationship between the elevation and area or elevation and storage. For the simulation to run it is necessary to state an initial condition which sets the amount of storage in the reservoir at the beginning of the simulation. One of the initial condition to choose from is the inflow = outflow. This condition takes the inflow to the reservoir at the start of the simulation, and either use the relationship between the storage and discharge to compute a same flow rate as outflow, or determines the pool elevation necessary to cause flow over the outflow structure. Elevation is an other initial condition, which can be used to interpolate the storage from the elevation-storage curve. The selected initial conditions and input parameters are presented in appendix 2.

The storage volume of the lakes are unknown. To be able to specified the relationship between the elevation and area for each of the lakes, it is been necessary to makes some assumptions. The solution has been to measure the surface

area of each of the lakes, and assumed constant area within the 2 m depth. Since the reservoirs are unregulated, the water will flow over the weir when the water elevation increases the level of the outlet structure. The water storage below this elevation of 2 m is assumed not to contribute to the runoff from the reservoir. If the water goes beneath this line, there will not be any outflow from the reservoir. Each of the dams has outlet orifices which will in reality contribute to the runoff. However, the condition and geometry of these pipes are unknown. The contributions of these to the runoff are therefore difficult to estimate. To ease the simulation the contribution of these has been neglected.

The simulations in HEC-HMS are divided into two models, one model developed for calibration and one is developed to simulate the runoff to Ilabekken. The model for calibration includes the catchment upstream of Kobberdammen. Since there is an observation site at Kobberdammen surveying the discharge gives opportunity to compare the simulated runoff directly to the observed. The selected method is the outflow curve method. Over the V-notch weir at Kobberdammen the relationship between the water level and discharge is possible to compute, by using equation 2.2 in section 2.3. The calibration process is more closely described in section 4.1.1.

Figure 4.1 shows the model layout of the whole catchment used in the simulation of the runoff to Ilabekken downstream of Theisendammen. The catchment area is 8.78 km^2, and has a difference in elevation ranging from 153 m.a.s.l at Theisendammen and up to 546 m.a.s.l. As the figure shows, the catchment is divide into three subcatchments. The catcment upstream of Kobberdammen is 0.82 km^2, subcatchment 2 is 4.92 km^2 and subcatchment 3 is 2.82 km^2.

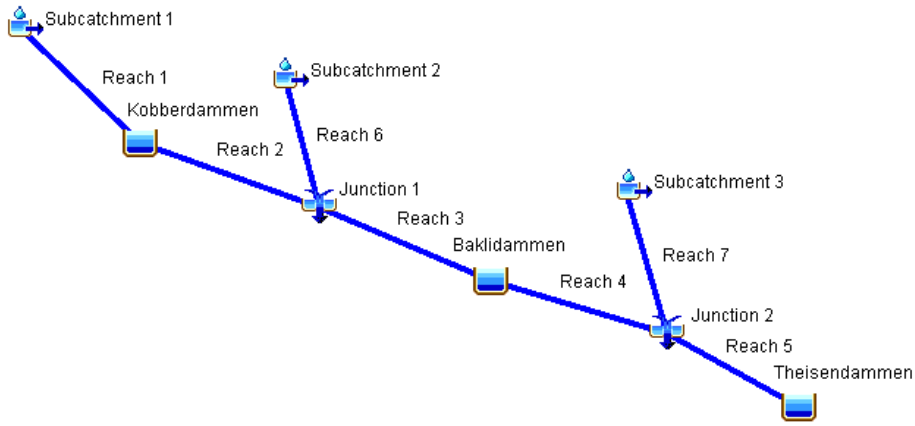

Figure 4.1: Model layout in HEC-HMS

An 200 years storm event is simulated for the whole catchment. The frequency storm method is used to produce a synthetic storm event computed by statistical precipitation data. The statistical precipitation data are the partial-duration depths which are the cumulative precipitation depths expected for the specified storm event. These values are presented in section 2.3. The intensity duration and the storm duration must be specified. The intensity duration is the shortest time period of the storm event, usually set equal to the time step of the simulation. The time step of the simulation is set to be 15 min. The time step of the simulation should be reasonably short, at least shorter than the precipitation data since the time series data are interpolated to the time interval during the simulation. The storm duration determines how long the precipitation will last. For the synthetic storm event in this simulation the storm duration is set to be 6 hours. The intensity position is selected to be 50 % which mean that the peak intensity will occur after 3 hours with a storm duration of 6 hours.

4.1.1 Calibration

Some of the input parameters in HEC-HMS can be determined directly from field measurements, such as catchment characteristics like the area of the catchment. Other parameters can indirectly be estimated by field measurements or experience. Parameters that cannot be estimated by observation or measurements must be calibrated. The aim of the calibration is to estimate the parameters that yield the best fit between the simulated runoff and the observed runoff at Kobberdammen. The calibration process will optimize a set of parameters, however process will not be a complete calibration since all of the model data are not included.

A schematic of the calibration process is shown in figure 4.2. To be able to optimize the best set of parameters it is necessary to select initial values. The better these initial estimates are, the quicker the calibration process will reach a sufficient result.

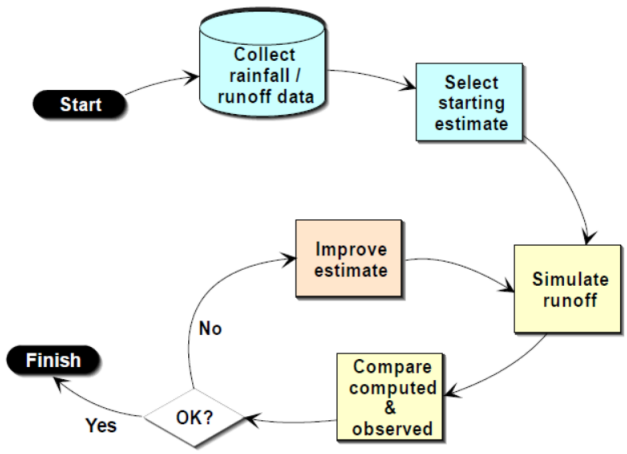

Figure 4.2: Schematic of calibration process, adapted from Bulcock and Jewitt [2010]

HEC-HMS includes a model optimization which makes it possible to estimate the parameters automatically. An objective function is the quantitative measure of how good the computed hydrograph correlate with the observed. The function equals to zero if it is an identical fit between the observed and simulated. One of the objective functions available are the peak-weighted RMS error function which weight flows above average most and gives less weight on flows below average. Since the peak flows are of most interest in this thesis, this objective function is chosen in the optimization.

A part of the meteorological model manager is the snow melt method which make it possible to simulate the processes including snow. To be able to simulate these processes the model requires several input parameters. Some of these parameters can be estimated by experience found in literature, while others must be estimated through calibration. It has been tried to include the snow melt process with estimated values in the model, however there has been a challenge to get the model stable. On the basis of this it has been chosen to calibrate the model from the start of June till the end of September to avoid the effect of snow melt. Three summer seasons have been simulated in the calibration process, to be able to compare the results.

Historical precipitation data are useful for calibration of model parameters. The time series used in the calibration are collected from Voll observation site described in section 2.3. The precipitation data are given for every 12 hour which means that the total volume within the last 12 hours are included. The time se-

ries for temperature are given for every hour, which gives the temperature at the specified time of measurement. It is assumed that these observations are representative for the catchment upstream of Kobberdammen, and to be uniformly distributed over the catchment. In the simulation the evapotranspiration must be specified. The monthly average has been chosen to use, which is computed by the equation 2.3 described in section 2.3. Evaporation is only included in the calibration process, since the the effect of evaporation is limited during a 200 year storm event.

4.1.2 Sensitivity Analysis

A sensitivity analysis determines which parameters have the greatest impact on the model result. A sensitivity analysis can either be global or local. In local sensitivity analysis the effect of each parameter is determined separately, while the set of parameters are held constant. In a global sensitivity analysis all model inputs can vary over their range at the same time [Cunderlik and Simonovic, 2004]. By using a sensitivity analysis, more attention can be given to the most sensitive parameters.

A local sensitivity analysis can be used to evaluate the impact the calibrated parameters have on the model result. The set of calibrated parameters have been considered as the baseline parameters. For each summer season the simulation has been run for the baseline parameters, while each of the parameters have been increased and decreased with 10 %, while the others have been held constant. The sensitivity analysis only considers the magnitude of the computed peak flow, and does not include the total volume or the timing of the peak. The greater the change in the peak flow, the more sensitive the model is to the particular parameter.

4.2 River Flow Simulations in HEC-RAS

HEC-RAS allows the user to perform one-dimensional steady and unsteady river flow simulations. In one-dimensional flow simulations the flow in x-direction is observed, while the flow in the y- and z-direction are ignored. This is normally a sufficient simplification since the lateral and vertical flow are generally much smaller than the longitude flow. One-dimensional systems assume a constant water stage in each cross section. To be able to compute flow simulations the model requires geometry of upper and lower cross sections which means the coordinates of each break point along the stream. For each cross section the model requires the distance from the left side (y-coord.), the bed elevation (z-coord.) and the distance to the downstream cross section (x-coord.). A basic conceptual element

in HEC-RAS is the channel segment between two cross sections shown in figure 4.3.

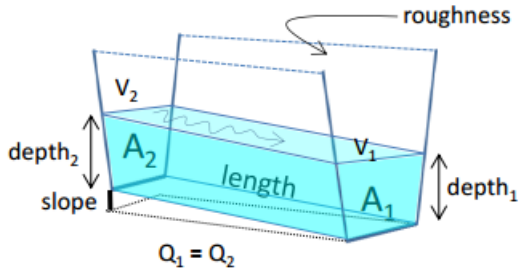

Figure 4.3: A basic conceptual channel segment between two cross sections, adapted from Rinde [2014]

Interpolation between the cross sections is often necessary to supplement the measured cross section data. The program can generate cross sections by interpolating the geometry between two known cross sections. Interpolation is often required when the change in the velocity head is too large to accurately compute the change in the energy gradient [Brunner, 2010]. The maximum distance between the interpolated cross sections is set to be 5 m which means that for at least each 5 m it is a computed cross section.

In a steady flow simulation the water surface profiles are computed from one section to the next by solving the energy equation. The steady flow data consist of boundary conditions, flow peak information and type of flow regime. The steady flow simulation is capable of model subcritical, supercritical or mixed flow regime water surfaces. Boundary conditions are necessary to establish the initial water level at both the upstream and downstream end of the river. Subcritical flow is downstream controlled which means that the downstream boundary condition must be specified because of backwater effect from downstream cross section. Supercritical flow is upstream controlled since there is no backwater effect from downstream sections and the upstream boundary condition must be specified. Mixed flow regime includes both subcritical and supercritical flow regime thus the boundary condition at each end of the river must be included [Rinde, 2014].

In this thesis steady flow simulations will be performed, using mixed flow regime. The selected downstream boundary condition is set to be the normal depth which required a friction slope that the program will used to calculate the normal depth at the location using Manning's formula presented in section 3.1. The upstream boundary condition is set to be the critical depth which the

program will compute for each of the profiles and use the result as the boundary condition. The discharge data from the hydrological model are entered at the upstream end of the reach. The flow remains constant along the stream since it is performed a steady flow simulation. The catchment downstream from Theisendammen which will contribute to runoff to Ilabekken is less than 1 % of the total catchment area upstream of Thesisendammen. The contribution of runoff from this area is neglected since the amount of water will be much smaller than the discharge from Theisendammen. In the calculation of critical depth the program use a Froude number of 0.94 instead of 1.0 due to inaccuracy in irregular channels [Brunner, 2010]. Using a value of 0.94 is therefore conservative, thus the program will calculate critical depths more often than it may need to.

To be able to develop a model with an acceptable accuracy it is important to survey cross sections which give a good fit of the physical river geometry. The river geometry has been surveyed with GPS measurement. It has been a challenge to complete the measurements at several places along the stream due to poor reception of the GPS signals and some locations with difficult excess. It has therefore been necessary to make some assumptions regarding the cross section. By using maps and photos from the area, have made it possible to estimate cross sections at the places with limited data. The modelled part of the stream is roughly 420 m long, and has an elevation difference of 42 m. An overview of the cross sections are shown in appendix 3. The coordinates measured with GPS were imported to ArcGIS which is a geographical information system making it possible to visualize geographical data. In ArcGIS the length between each coordinate was measured manually, producing the river geometry which were exported to HEC-RAS.

An alternative to this approach is to use HEC-GeoRAS which is a ArcGIS extension specially designed to process geospatial data to use with HEC-RAS. The interface allows the preparation of geometric data for import to HEC-RAS from an existing digital terrain model [Ackerman, 2009]. Since it was no available digital terrain model in the area, the import of the coordinates to the river model was not conducted with this program. The design discharge in the simulation is set to be the 200 years flood with an increase of 20 % to include the effect of climate change, as described in 2.3.1. For constructions in areas exposed for flooding the requirement for the design flood is often set to be a 200 year event, which represents the requirement of the flood level in the safety class with medium consequence presented in TEK10 [Direktoratet for byggkvalitet, 2010]. There will also be conducted simulations of the 200 year flood, and with increase of 40 %. This make it possible to investigate the effect the different flood magnitudes will have on the flow pattern in Ilabekken.

4.2.1 Choice of Manning's Roughness Coefficient

An important parameter in HEC-RAS is the Manning's roughness coefficient, the n-value, which is used to reflect the water resistance to flow in the river sections. In natural irregular channels the roughness will vary over the cross section. In HEC-RAS the cross sections are subdivided into three part by specifying the left and right bank stations. A constant roughness coefficient must be specified for the subdivided parts of the cross section. In reality, the roughness coefficient is highly variable and is effected by several factors. Vegetation may variate throughout the year, giving a higher roughness when vegetation is high. The effect of the vegetation will depend on type of vegetation, distribution, height and density [Te Chow, 1959]. Since it is a continuous change in the natural streams due to erosion, sediment transport and deposition the cross sections will variate. The n-value will increase as a result of the energy used in eroding and transporting the material. In most streams the roughness will decrease with increasing stage and discharge. Flood plains has generally larger roughness than the main channel due to more water resistance to flow.

It is no exact method to determinate the Manning's roughness coefficient, this can be done by calibration or by selecting suitable table values based on previous experiments. In general the n-values should be calibrated by comparing the observed water level with the simulated, at a specific runoff to be able to optimize the roughness coefficients. Calibration of the HEC-RAS model has not been conducted in this thesis. The roughness coefficients are therefore selected from literature and experience. Selected n-values for the stream studied in this thesis are shown in table 4.1 where the left overbank is referred to as LOB and the right overbank as ROB. These values are based on n-values presented in the book *Open Channel Hydraulics* by Te Chow [1959] which shows n-values for various types of channels. This can an useful guidance to select suitable n-values when limited data is available.

A sensitivity analysis can be performed to evaluate the model sensitivity to variations in the Manning's roughness coefficient. The procedure involves holding the other model parameters constant while changing the n-values.

Cross section	n-value LOB	n-value Channel	n-value ROB
29	0.020	0.020	0.020
28	0.050	0.045	0.040
27	0.050	0.045	0.040
26.5 Bridge			
26	0.050	0.045	0.040
25	0.050	0.045	0.050
24 V-notch weir			
21	0.070	0.045	0.070
20	0.070	0.045	0.070
19	0.070	0.045	0.070
18	0.070	0.045	0.070
17	0.070	0.045	0.070
16	0.040	0.045	0.070
15	0.070	0.045	0.070
14	0.070	0.040	0.070
13	0.060	0.050	0.060
12	0.060	0.050	0.060
11	0.060	0.050	0.060
10	0.060	0.050	0.060
9	0.060	0.050	0.060
8	0.060	0.050	0.060
7	0.060	0.050	0.060
6	0.060	0.050	0.060
5	0.060	0.050	0.060
4	0.060	0.050	0.060
3	0.060	0.050	0.060
2	0.060	0.050	0.060
1 Inlet culvert	0.060	0.020	0.060

Table 4.1: Selected Manning's n-values for the different cross sections

Chapter 5

Results

5.1 Calibrated Values in HEC-HMS

Calibration of the HEC-HMS model has been conducted in order to optimize the correlation between the simulated runoff and observed runoff from Kobberdammen. The calibration process includeds a set of ten different parameters. Table 5.1 shows the calibrated values of different input parameters.

Parameter description	Calibrated value
Constant loss rate [mm/hr]	0.13
Initial loss [mm]	0.20
Max canopy storage [mm]	3.4
Initial canopy storage [%]	30
Max surface storage [mm]	0.20
Initial surface storage [%]	50
Lag routing [min]	99.9
Time of concentration [hr]	3.4
Storage coefficient [hr]	1.5
Baseflow $[m^3/s]$	0.01

Table 5.1: Calibrated values in the HEC-HMS model

The simulated outflow compared with the observed through the summer of 2011, 2012 and 2013 are shown respectively in figure 5.1, figure 5.2 and in figure 5.3. The best correlation is obtained for the simulation during summer of 2012. For this simulation the correlation between the peak flows is approximately the same. The simulated peak flow is 0.148 m^2/s while the observed peak flow is 0.147

m^2/s, which gives a difference of 0.3 %. The time of peak for the simulated is at 04:30 8th of September while the observed peak flow occurred at the same date at 09:00. The simulated volume is roughly 52 percent more than the observed. From the mid-June till the start of September the simulated runoff is generally over-predicted compared with the observed.

The match between the greatest simulated and observed peak flow for the summer of 2011 is not quiet as good as the one for 2012. The graph shows that the hydrographs follow the same trend, but the magnitude of the highest peaks are different. The greatest simulated peak flow occurs at 12th of September and has a magnitude of 0.211 m^2/s. The corresponding observed peak flow is 0.095 m^2/s, which gives a peak flow difference of 55 %. In this simulation the correlation between the outflow volume has only a difference of 0.8 %, with the observed volume being slightly higher than the simulated.

The simulation of the summer of 2013 the hydrographs do not correspond as well as for the other summer seasons. The simulated flow is located more to the left compared with the observed. The magnitude of the peak flow in August is not captured in the simulation, while in September the model simulate a peak flow which is not observed. The greatest peak flow observed occurs at 13th of August and has a magnitude of 0.132 m^2/s. The corresponding simulated peak flow occurs earlier at the same date and has a magnitude of 0.070 m^2/s, which represent a difference of 47 %. The difference in volume is around 17 %. Even though the hydrographs are displaced compared to each other and the size of the flow peaks are different, the simulation shows a trend of the correspondence between the simulated and observed outflow.

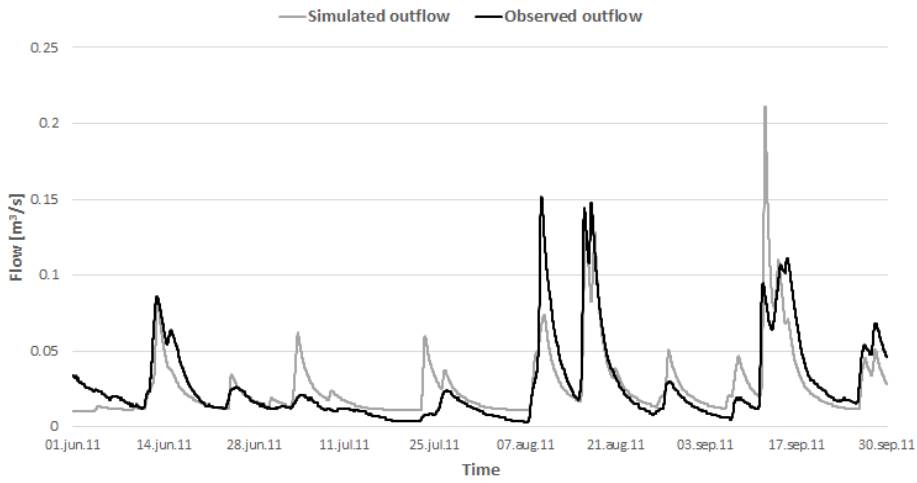

Figure 5.1: Comparison of simulated and observed outflow from Kobberdammen at summer 2011.

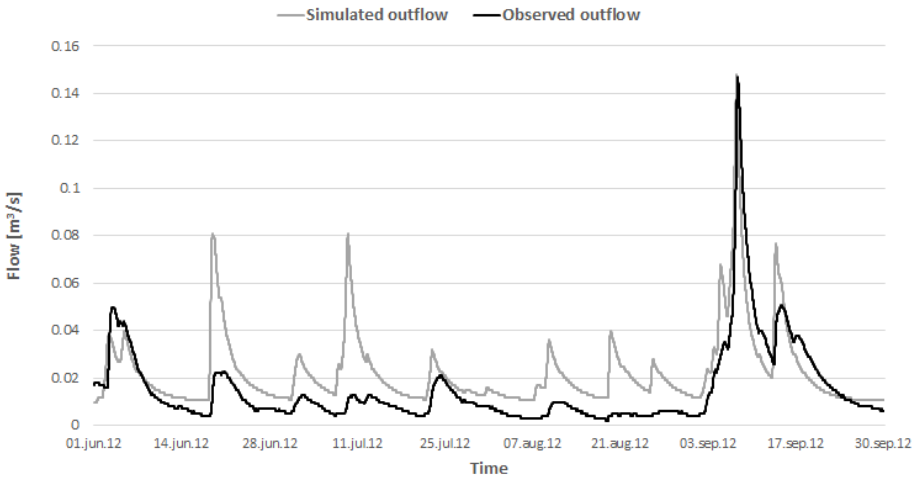

Figure 5.2: Comparison of simulated and observed outflow from Kobberdammen at summer 2012.

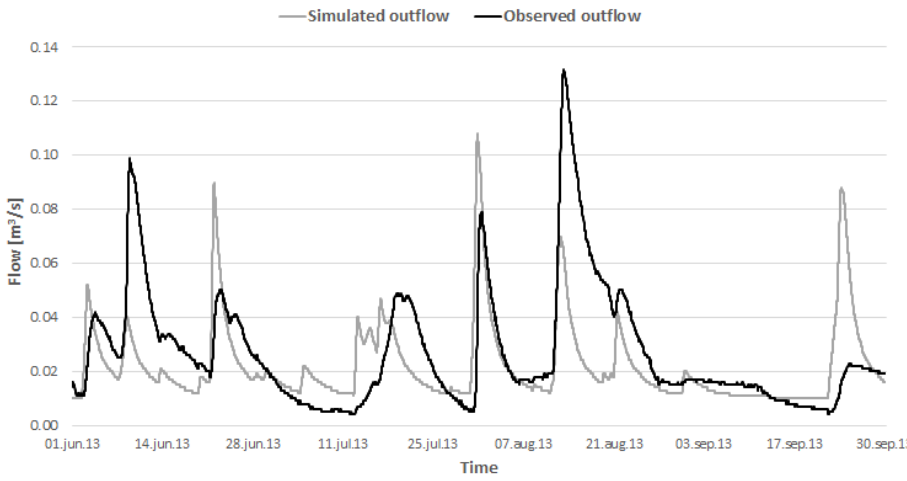

Figure 5.3: Comparison of simulated and observed outflow from Kobberdammen at summer 2013.

5.1.1 Sensitivity Analysis of the Calibrated Parameters

A local sensitivity analysis has been adapted to evaluate the influence the set of calibrated parameters have on the model result. Of the 10 different parameters which are subject for the sensitivity analysis, half of the parameters are influencing the model result when changing their values with ± 10 %. These parameters are the constant loss rate, the maximum canopy storage, the time of concentration, the storage coefficient and the base flow. The highest differences between the magnitudes of the peaks are caused by altering the constant loss rate and the base flow, presented in table 5.2 and in table 5.3. The other parameters are influencing the model result on a smaller scale, these are given in appendix 2.

Table 5.2 shows that when the constant loss rate increases the peak flow decreases for all of the seasons, whereas when the constant rate decreases the peak flow increases. The greatest percent error in peak flow is 2.78 % when the constant rate is increased in the model of summer 2013. When the base flow increases the peak flow increases, whereas the peak flow will decrease with decreasing base flow, as shown in table 5.3. The greatest change in the peak flow is when the base flow is decreased in the summer 2013, the error in peak flow is then 2.78 %.

	Parameter change [%]	Constant loss rate [mm/hr]	Simulated peak flow [mˆ3/s]	Peak flow change [%]
Summer 2011	10	0.143	0.208	1.42
	0	0.130	0.211	0.00
	-10	0.117	0.213	0.95
Summer 2012	10	0.143	0.144	2.70
	0	0.130	0.148	0.00
	-10	0.117	0.151	2.03
Summer 2013	10	0.143	0.105	2.78
	0	0.130	0.108	0.00
	-10	0.117	0.110	1.85

Table 5.2: Sensitivity analysis of the constant loss rate

	Parameter change [%]	Base flow $[m^3/s]$	Simulated peak flow $[m^3/s]$	Peak flow change [%]
Summer 2011	10	0.011	0.214	1.42
	0	0.010	0.211	0.00
	-10	0.009	0.208	1.42
Summer 2012	10	0.011	0.149	0.68
	0	0.010	0.148	0.00
	-10	0.009	0.146	1.35
Summer 2013	10	0.011	0.110	1.85
	0	0.010	0.108	0.00
	-10	0.009	0.105	2.78

Table 5.3: Sensitivity analysis of the base flow

5.2 Hydrographs Generated with HEC-HMS

By applying the values of the calibrated parameter presented in section 5.1 to be representative for the whole catchment upstream of Ilabekken, the hydrological response can be simulated.

Figure 5.4 shows the simulated inflow and outflow curve of the 200 year flood event (Q_{200}) at Theisendammen. The peak of the outflow is simulated to be 17.14 m^3/s, and will occur approximately 14 hours after the start of the storm event. The inflow to Theisendammen has the highest peak of 18.59 m^3/s occurring after 13 hours. This shows that the magnitude of the runoff will be damped in Theisendammen with 1.45 m^3/s and the peak flow will be delayed with 1 hour.

To including the effects of climate change the magnitude of the resulting hydrograph is increased with 20 and 40 %, shown in figure 5.5. The increase of 20 and 40 % gives a peak flow of 20.57 m^3/s and 24.00 m^3/s, respectively.

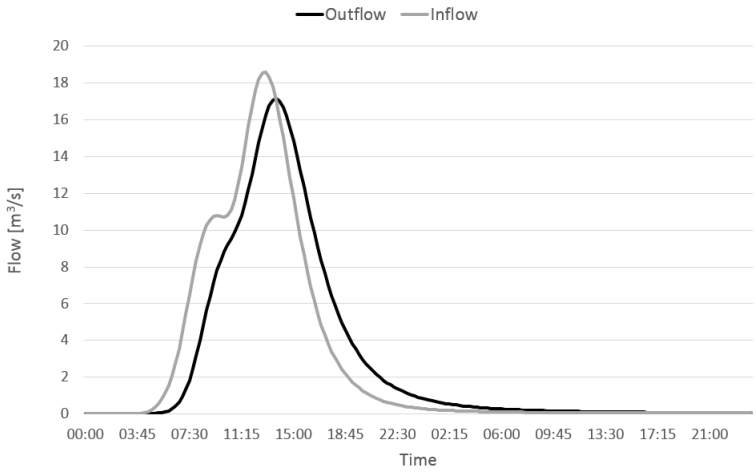

Figure 5.4: Inflow and outflow curve of Q_{200} at Theisendammen

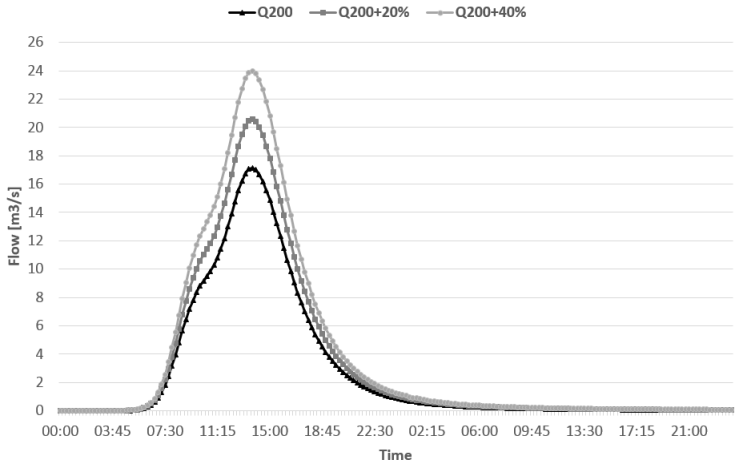

Figure 5.5: Outflow curve of Q_{200} from Theisendammen with an increase of 20 and 40 %

5.3 Simulation Results from HEC-RAS

There have been performed simulations of three different flood scenarios, the 200 year flood, Q_{200}, the 200 year flood with an increase of 20 %, $Q_{200+20\%}$, and the 200 year flood with an increase of 40 %, $Q_{200+40\%}$. Figure 5.6 shows the change in water stage and the variation in flow regimes in the longitudinal section of Ilabekken at $Q_{200+20\%}$. The dotted green line indicates the energy grade line (EG), the blue solid line shows the water stage (WS) and the red line with markers present the critical flow (Crit). The flow direction goes from right to left, as the outlet of Theisendammen is at elevation 153 m.a.s.l and located 420 m along the main channel.

As figure 5.6 shows, supercritical flow regime dominates at the start of the reach as the water stage is below the critical line. Downstream of the outlet the difference in the energy grade line and the water level indicates higher velocity here than in the rest of the stream line. In the last 80 m of the simulation reach, the water stage increases and the flow regime becomes subcritical. As the figure indicates, hydraulic jumps will occur at approximately 370 m (at cross section 25) and 260 m (at cross section 17) from the end of the simulated reach. Here the flow changes from supercritical to subcritical, the plot show clearly a sudden increase in the water stage and a decrease in the flow energy. The cross section 25 is upstream from the V-notch weir located in the stream, which shows that the structure will affect the flow pattern. Cross section 17 is located upstream from a old stone wall which narrows the width of the channel.

Since $Q_{200+20\%}$ is set to be the design flow in this thesis the simulation results of this discharge plot is presented. The longitudinal profiles for each of the flood scenarios show the same trend in variation in flow regimes as in figure 5.6, however with a difference in water stage elevation. These are given in appendix 3.

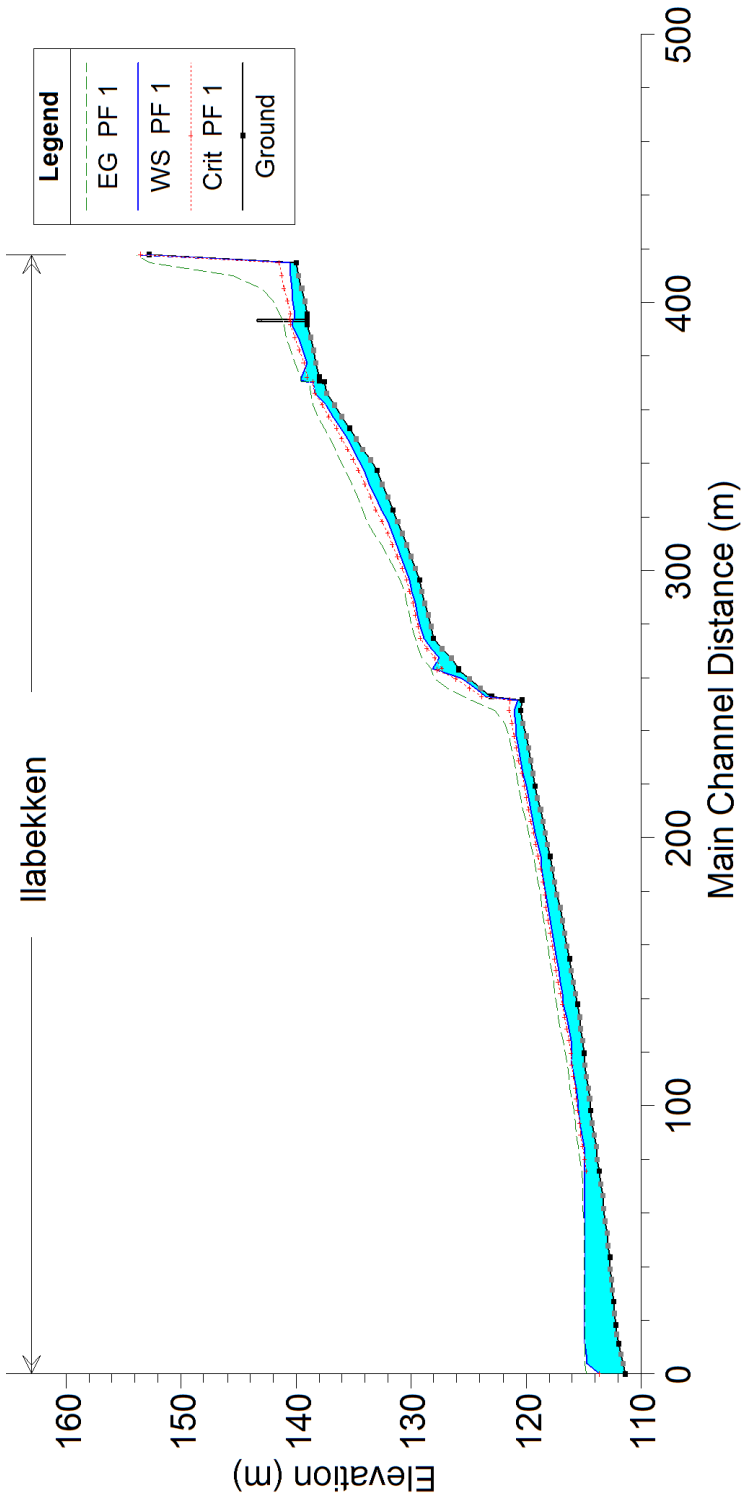

Figure 5.6: Longitudinal profile plot of $Q_{200+20\%}$

Figure 5.7 shows an overview of modelled part of Ilabekken after the simulation of the design discharge. The blue solid illustrates the water stage during the peak flow and the red dots shows the bank stations which indicates the boundary of the main channel. The cross sections are identified with numbers. The cross sections labeled with * are the interpolated cross sections. As the figure shows, the water stage exceeds the main channel boundary at most of the cross sections. In the last 80 m of the modelled reach, the right overbank will specially be flooded. At cross section 4 the water flows 16.5 m across the right floodplain. The culvert at the end of the reach will in all of the simulated flood scenarios have enough capacity to obtain open flow at the inlet. The water stage elevation at the inlet of the culvert during each of the flood scenarios are given in appendix 3.

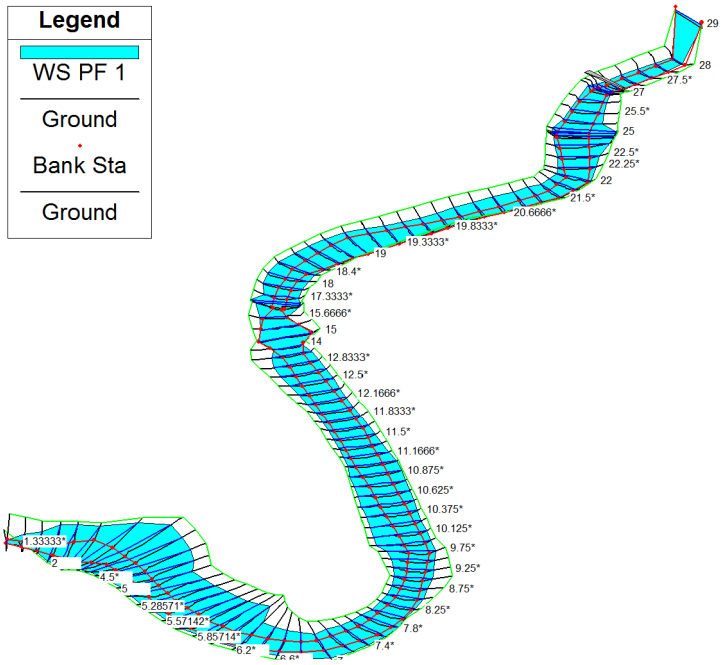

Figure 5.7: Perspective plot of Ilabekken

Figure 5.8 and figure 5.9 show the velocity and shear stress in the main channel at the simulations with the three flood scenarios. Downstream the outlet of Theisendammen occurs the highest velocity as figure 5.8 shows. As the figure indicates there is no significant difference between the velocities, the velocities here are almost 16 m/s. Further downstream the velocity at $Q_{200+40\%}$ will be

faster than the others in the steep part of the stream. The velocity plot shows clearly the hydraulic jumps at cross section 25 and 17 due to a sudden decrease in the velocity. At approximately 250 m upstream of the reach end, the velocity first increases and then suddenly decreases. In this part of the stream it is a steep fall as the longitudinal profile in figure 5.6 shows, producing high velocities. In the part of the stream between 40 and 85 m a long the channel the velocities changes, and the velocity at $Q_{200+40\%}$ slows down more rapidly and goes below the other velocities. The velocity at Q_{200} is not decreasing so fast, and here the water will flow fastest compared with the other scenarios.

Figure 5.9 shows the difference in shear stress in the main channel produced by the flood events. The greatest shear stress occurs downstream of the outlet of Theisendammen, here the shear stress produced by Q200 gives the highest values. Further down the shear stress produced by $Q_{200+40\%}$ will be slightly higher than the others, however there is no significantly difference between the three scenarios. As figure 5.9 indicates, the shear stress of $Q_{200+40\%}$ decreases 85 m before the end of the reach and goes below the two other scenarios.

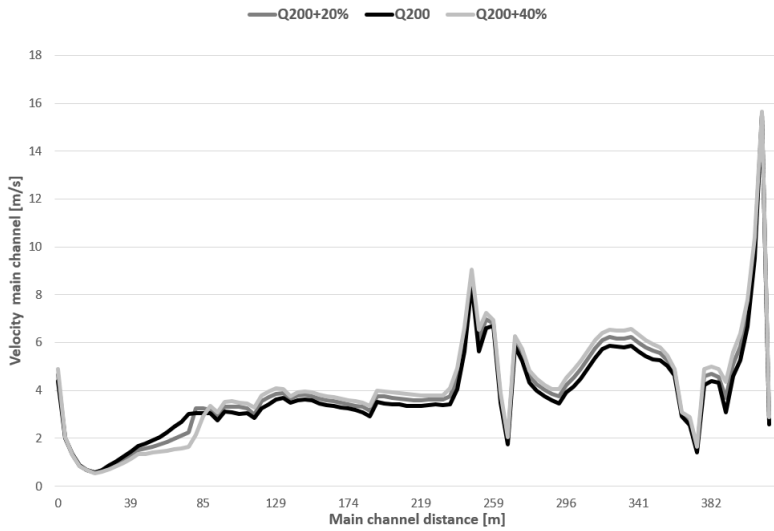

Figure 5.8: Velocity in main channel along the the stream line for the different flood scenarios

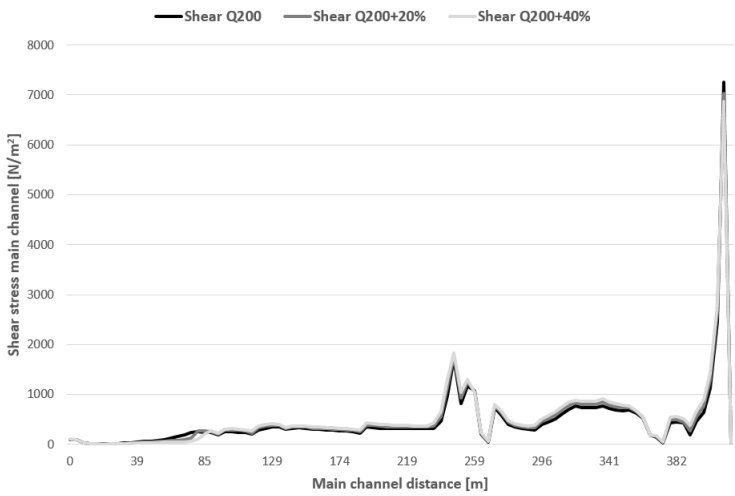

Figure 5.9: Shear stress in main channel along the the stream line for the different flood scenarios

5.3.1 Computation of Stable Stone Size

To estimate the stable stone size in specific parts of the stream the Shields equation and the HEC-11 method as described in section 3.3 are used.

The parts of the stream which are expected to be most exposed to erosion are evaluated based on the theory of erosion processes described in section 3.2, and the result from the simulations in HEC-RAS. Cross sections evaluated to be exposed to erosion are presented in figure 5.10. Cross section 22 is located in a curve downstream of the V-notch weir, which will induce high velocities in this part of the stream. The results of the simulations show high velocities in the area where cross section 18 is located. Cross section 12 is selected since the velocity against the river bank is high and that observations show that this area is exposed to erosion. Picture taken during the field measurements is given in appendix 4. Several cross sections in the sharp bend are selected to investigated the stability in the lateral bend. To be able to investigate how the decrease in velocity and shear stress will affect the size D_{50}, cross section 6.2* is included in the computation.

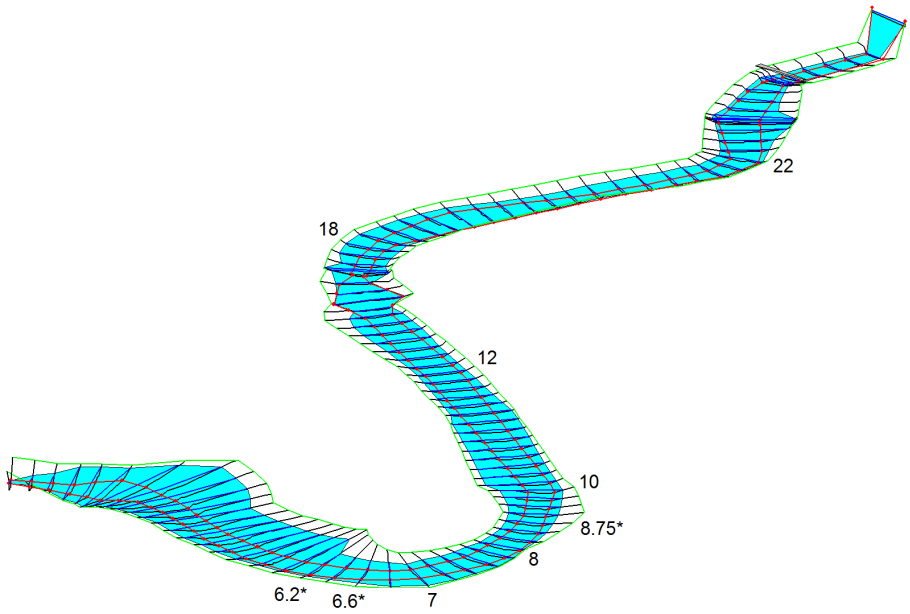

Figure 5.10: Selected cross sections exposed for erosion

Table 5.4 shows the computed D_{50} with Shields equation for the different flood scenarios at the selected cross sections. The table also includes the percentage change in D_{50} between the Q_{200} and the $Q_{200+40\%}$. When the magnitude of the flow increases with 40 % the corresponding change in stable stone size gives smaller increase. Of the selected cross section, the computed D_{50} in cross section 8 gives the highest increases with 26.9 % when the magnitude of the flood increases with 40 %. The D_{50} computed by HEC-11 method for the different flood scenarios at the selected cross sections are presented in table 5.5. With this method the change in the flood magnitude gives greater difference in the size of D_{50} than with Shields equation. The change in the stable stone size at cross section 8 differs with 45.4 % between Q_{200} and the $Q_{200+40\%}$.

As the tables indicate the computed D_{50} varies between the two methods. Especially at cross section 22, 18, 12 and 10 the difference is marked. In cross section 18 the estimated D_{50} at Q_{200} for HEC-11 is more than 11 times larger than for Shields. At cross section 6.2* the percentage change between the Q_{200} and the $Q_{200+40\%}$ give a decrease in the stable stone size of 59.5 % with Shields and 71 % with HEC-11. In the cross sections where the side slope is more not so steep, the methods correspond better.

The input parameters to the computation of the stable stones sizes and plots of each cross sections are given in appendix 4.

	D_{50} [m] computed with Shields			Change [%] between
Cross section	Q_{200}	$Q_{200+40\%}$	$Q_{200+40\%}$	Q_{200} and $Q_{200+40\%}$
22	3.35	3.6	3.79	13.1
18	2.26	2.47	2.67	18.1
12	0.88	0.97	1.05	19.3
10	0.96	1.04	1.12	16.7
8.75*	0.82	0.88	0.93	13.4
8	0.78	0.9	0.99	26.9
7	0.73	0.79	0.87	19.2
6.6*	0.7	0.75	0.79	12.9
6.2*	0.79	0.84	0.32	-59.5

Table 5.4: Computed D_{50} with Shields at different discharges, and percentage change between Q_{200} and $Q_{200+40\%}$

	D_{50} [m] computed with HEC-11			Change [%] between
Cross section	Q_{200}	$Q_{200+20\%}$	$Q_{200+40\%}$	Q_{200} and $Q_{200+40\%}$
22	6.07	6.84	7.48	23.2
18	25.55	29.3	32.93	28.9
12	6.13	7.16	8.07	31.6
10	1.44	1.63	1.83	27.1
8.75*	0.89	0.96	1.09	22.5
8	1.08	1.35	1.57	45.4
7	0.41	0.49	0.56	36.6
6.6*	0.44	0.49	0.53	20.5
6.2*	0.62	0.73	0.18	-71.0

Table 5.5: Computed D_{50} with HEC-11 at different discharges, and percentage change between Q_{200} and $Q_{200+40\%}$

5.3.2 Sensitivity Analysis of Manning's n-values

A local sensitivity analysis has been adapted to evaluate the influence variations in the roughness coefficient haa on the water stage elevation at each of the cross sections. The simulation of $Q_{200+20\%}$ has been run with n-values varying by $\pm$ 25 % relative to the selected n-values presented in section 4.2.1. Table 5.6 shows

the percentage change in the water stage elevation (WS), relative to the selected n-values when these are multiplied with 0.75 and 1.25. As the table indicates, the water stage elevation increases with increasing roughness coefficient. The greatest change occurs at cross section 27. When the n-values in this profile increase with 25 %, the change in the water stage elevation is 60.9 %. The sensitivity of changing the n-values differs between the cross sections, in some of the cross section the water level does not change with changing roughness. The change in the n-values of $\pm$ 25 % gives for most of the cross sections smaller degree of change in the water level.

	Change in WS [%]	WS [m]	Change in WS [%]
Cross section	n x 0.75	n	n x 1.25
29	0	0.75	0
28	0	0.56	0
27	-19.2	1.10	60.9
26	-27.7	1.37	8.8
25	0	1.47	0
23	0	1.02	8.8
22	-7.8	0.77	7.8
21	-7.5	1.07	7.5
20	-11.1	1.08	9.3
19	-10.1	0.79	10.1
18	-12.9	0.93	10.8
17	0	2.30	0
16	0	1.93	0
15	-9.1	0.44	9.1
14	-4.3	0.46	6.5
13	-14.8	0.61	14.8
12	-15.2	0.79	13.9
11	-12.3	0.81	11.1
10	-13.4	1.12	8
9	-15.3	1.24	10.5
8	-13.3	1.05	18.1
7	-12.4	0.97	16.5
6	-27.5	1.31	8.4
5	-1.4	2.13	1.9
4	-1.2	2.46	1.2
3	-0.8	2.66	1.1
2	-0.7	2.94	1.0
1	0	2.30	0

Table 5.6: Sensitivity analysis of the n-values, with respect to water stage elevation

Chapter 6

Discussion

6.1 The Future Climate in Trøndelag

Since the report *Klima i Norge 2100* was developed in 2009, the emission scenarios and the global climate models have been modified. The newest scenarios are comparable to the emission scenarios in the IPCC report from 2007. By using the report from Norway to evaluate the climate effects in Trøndelag it is important to specify that the results are not based on the newest data available. Since this thesis does not include downscaling of the global climate models, the Norwegian report is basis for the discussion of possible consequences of climate changes in Trøndelag.

The projected results which are applicable for Trøndelag presented in section 2.1.1, shows significant differences between the three scenarios. This illustrate the uncertainties regarding the future climate, however these values give an indication on how the climate change will be in this region. The findings in the report illustrate the season variations in Trondheim. The largest increase in temperature is during the winter months. This implies that temperatures around zero degrees Celsius will occur more often, leading to more freeze thaw cycles. A consequence to this is less amount of snow in the catchment during the winter, which could mean that the large spring floods will decrease in size as a result of lower snow melt. The floods can occur more often during the winter and spring, but at a smaller scale as a result of a more even snow melt through the winter season. The largest combination floods where snow melt and heavy precipitation occur at the same time can be reduced. In the period from 2071 till 2100 the greatest increase in the amount of precipitation is predicted to come during the autumn for the medium and high scenario. The change in the amount of precipitation varies greatly between the scenarios. The low scenario gives only an increase of

0.9 % in the precipitation amount during the autumn, while the high scenario gives an increase of 60.8 %.

The values presented in table 2.2 in section 2.1.1 show a main trend of an increase in number of days with lots of precipitation, and an increase in the magnitude of precipitation at these days. These values do not tell if the magnitude of the largest flood events will increase. However, with more precipitation occurring more often will accumulate more water in the hydrological system leading to more water available for runoff. This can imply a tendency of more extreme weather in the future. The highest increase in the days with lots of precipitation will occur during the autumn season according to the results. These results indicate that floods during the autumn season will most likely occur more often and at a larger scale in the future due to more precipitation.

6.2 Hydrological Considerations

The hydrological model can only make an impression of the physical catchment, as mathematical models never will match a physical system exactly. The quality of the results of the model will be influenced by the quality of the data and processes in the model. It is therefore important to be aware of the basis of the model, the assumptions which have been taken and the accuracy and quality of the input data. It is not always curtain that a 200 year precipitation event, P_{200} will yield a 200 year flood, Q_{200}. This will depend on the initial condition of the catchment at the start of the storm event as described in section 2.2. In the thesis there is assumed that P_{200} will produce Q_{200}. The magnitude of the computed Q_{200} depends on the choice of storm event duration. The duration of a design storm often correspond to the concentration time for the whole catchment. An roughly estimate of the time of concentration in the catchment give a value of 4 hours. Since the calibrated values of the time of concentration give higher values, the storm event duration is set to be 6 hours.

As described in the results in section 5.2 Theisedammen will contribute to an decrease in the magnitude of peak flow and delay the time of peak. The lakes in the catchment will contribute to a natural damped effect on the runoff. The modelled reservoirs in the HEC-HMS model will have some limitations since the storage volume of the lakes is unknown. The HEC-HMS model established in this thesis can be useful in evaluation of flood risk and change in future land-use in the catchment upstream of Ilabekken. A case of increasing urbanization in the area, will imply an increase in the impervious surfaces in the catchment, which can result in a faster and larger runoff from the catchment. In this type of scenarios the hydrological model can perform simulation while changing the percentage part of impervious surfaces in the catchment. The model can therefore be a tool used in management planning.

6.2.1 Consideration to the Calibration Process

The calibration of the HEC-HMS has been conducted by comparing the simulated runoff with the observed during three summer seasons. As descried in section 4.1.1 it has been a challenge to get the model to run while including the snow melt process. It has been tried to change the estimated input parameters, without success. It has been determined that it was more important to continue with the main topics in the thesis, and focus on obtaining a sufficient correlation for the summer seasons. It has been concluded that it will be acceptable to calibrate against the summer months as the snow melt normally is finished by the start of June, and the snow fall has not started by the end of September.

The calibration results presented in section 5.1 show the correlation between the simulated and observed runoff from Kobberdammen varies between the summer seasons. The best correlation between the flow peaks is obtained for the summer of 2012. From mid-June to the end of August, the simulated runoff are slightly over-predicted. A reason for this could be too high estimated base flow. By trying to decrease the base flow the correlation between the flow peaks become less accurate, as shown in the sensitivity analysis. It is therefore chosen to use the calibrated value of the base flow. However, to assume a constant base flow throughout the year will result in some errors since the base flow in the physical system will probably not be constant. The correlation for peak flows during the summers of 2011 and 2013 is less accurate than for the 2012 season. It can be several reasons why the set of parameters gives different correlation for the summer seasons. One of the main reasons considered to influence the correlation between simulated and observed runoff, is the fact that the observed precipitation used in the model is not from the actual catchment area. The observation site at Voll is located on a lower elevation and roughly 5 km away from the catchment. Across Trondheim precipitation could vary a lot. Short-term extreme precipitation can vary over short distances, hence the fallen precipitation at Voll can be greatly different from the precipitation in the catchment studied. The elevation difference between the catchment and the observation site can also contribute to the variations between the simulated and observed runoff. As temperature often will decrease with increasing elevation, the actual evaporation can be lower than calculated. This elevation difference has not been correlated for in the computation of the potential evaporation. If the calculated evaporation is too high, the simulated runoff in the catchment will be too low. An other reason for the differences may have something to do with the fact that snow melt is not included in the calibration. Snow melt can affect the water storage in the catchment after May, leading to higher discharge later in the summer.

The calibration process has difficulties to obtain good fit between both the base flow and the peak flows. When the physical system is adapted to a mathematical model, it will be difficult to obtain a good fit both at the low values

and at the same time correlate with the extremes. It will therefore be hard to obtain correlation in both volume and for peak flows at the same time. It has been attached most importance to have correlation between the flow peaks as the flooding events are of interest. Since the correlation between the summer seasons varies, it has been a challenge to find a set of parameters which correspond equally for each year. The choice has been to take basis in the calibration of summer 2012. This set of calibrated parameters are assumed to give a sufficiently fit of the processes in the catchment.

The time of concentration and storage coefficient can be computed from equations which depend on the catchment characteristics such as the length of the main channel and the catchment slope. The calculated values gave much small values compared with the optimized values in the calibration process. Since the calibrated values gave the best fit between the simulated and observed runoff, these values has been used further in the simulation of Q_{200}. Since the time of concentration and storage coefficient depends on the catchment characteristics these values will in reality not be the same for all of the subcatchments. However, since the calculated values for the catchment upstream of Kobberdammen did not correspond with the calibrated values, it is decided to used the calibrated values for the two subcatchments downstream from Kobberdammen. If the time of concentration increases, the runoff will be more damped in the catchment. Since subcatchment 2 and 3 are larger than subcatchment 1, the time of concentration in these catchments will probably be higher. If these values is set to be equal to the calibrated value, it will imply a faster runoff from the catchment than it actually will be. It is therefore assumed to be acceptable to use the same values for all the subcatchments.

6.3 Considerations of a Changed Flow Pattern

The results from simulations in HEC-RAS indicate that the different flood scenarios will contribute to variations in the flow pattern along the stream. The occurrence of hydraulic jumps in the stream indicates release of energy, which can contribute to erosion downstream. The areas downstream of the hydraulic jumps can therefore be exposed to erosion. The water will flood over the stream banks in each of the flood scenarios, and specially at the end of the model reach. Here the slope of stream channel decreases, leading to reduction in the flow velocities as shown in the results. The inlet of the culvert at the end of the reach will lead to a narrowing of the water flow, which leads to a increase in the water stage elevation.

A source of error in the HEC-RAS model is the inaccuracy in the river geometry. Since the surveying cross sections only express some parts of the river, the model will just give an indication of the physical river geometry studied.

Interpolation of the cross sections will give average cross sections between two measured profiles. In the physical stream this will not be the case, as natural streams will have irregular cross sections. Since there will be not practical or almost possible to measure the whole river geometry, it is important to focusing on surveying the most influencing parts. Since some of the cross sections have been estimated by use of observation and maps, this will contribute to an extra inaccuracy in the model. As shown in the sensitivity analysis of the n-values in the HEC-RAS model the roughness coefficients will influence the water levels in the stream. In some part of the stream the model is highly sensitive to change in the n-values, as the water stage elevation changes greatly. Use of the selected n-values without performing a calibration, the model will produce results with some errors and uncertainties.

In the computation of the stable stone sizes the selected cross sections evaluated give an indication on where the erosion could occur, however there could be other places exposed to erosion along the stream. The Shields equation and HEC-11 method are selected on the basis that the required input parameters are given by the simulation with HEC-RAS. The depth used is the HEC-11 method is the difference between the water stage and the minimum elevation in each cross section. This has been done since the difference between the maximum depth and the average depth is small and it is more practical to use the maximum depth since this is an output value in HEC-RAS. As the velocity will vary over the cross section of the river, local velocities can be very different from the average value. In outer bends and in deep parts of the river the velocity is usually higher than in shallow parts. The computation of stable stone size will only give a rough estimate. The computed D_{50} shows a great difference between the methods. In the HEC-11 method, the effect of the side slope is much larger than for the Shields equation. The effect of the stability in side slopes in the HEC-11 method depends on the ratio between the angle of repose and the angle of the side slope. If the side slope angle approach the angle of repose, the expression under the fraction line will converge to zero, resulting in a strong increase in the D_{50}. The choice of angle of repose will therefore influence the result greatly. As shown the cross section 18, the computed stable stone size is unlikely large. In this cross section the side slope angle is almost the same as the selected angle of repose.

The difference between the D_{50} computed with different discharges for Shields, shows that the change between the computed D_{50} with Q_{200} and $Q_{200+40\%}$ result in a change smaller than 40 %. This indicates that the stable stone size will not change in the same degree when the magnitude of the runoff increases. The results show that an increase in the runoff actually decreases the stable stone size in cross section 6.2*. When the magnitude of the flood increases, the water stage elevation will increase when the velocity decreases at shallow parts. In this thesis there is only evaluated particle erosion, which will only be one factor contributing

to the overall erosion process. One the basis of the computation of stable stone sizes, types of erosion protection measures can be evaluated. The choice of type of erosion protection depends one several factors, including the assets exposed of erosion, the cause of erosion, physical conditions in the stream and the area available [Jenssen and Tesaker, 2009]. Protection of exposed areas in a stream are often done with a stone layer. In the areas with steep side slopes a solution could be to establish a retaining wall of stones along the exposed area, which can be build almost vertically. It is often desirable to establish erosion protection measures which becomes a part of the environment in the stream. To maintain a natural surrounding, it is often desirable to use stones in the erosion protection measurement.

A changed flow pattern in the upper part of Ilabekken could cause possible consequences in the lower part over stream. With increasing runoff in the stream due to the climate change, the risk of flooding and erosion at the lower part will increase. Transport of sediments can lead to sedimentation in the lower parts of the stream where the velocity decreases due to more shallow areas. It is already observed sedimentation in the reopening part as described in section 1.1. Without any efforts upstream this will continue in the future. Sedimentation in the reopening part could lead to poorer condition for fish spawning in the area as the spawning ground could be filled up by sediments and mud. This could also affect the quality of the water and lead to consequences for the biological diversity in the area. Since lots of resources have been used to create a stream with biological diversity, high hydraulic capacity and with nice esthetically surroundings in the reopening part of Ilabekken, it is of interest to maintaining this condition. This can be done by focusing on efforts upstream the river, for instance establishment of erosion protection measures can be evaluated. Often can efforts upstream in a river systems prevent problems with erosion, sedimentation and flooding downstream in the river.

Chapter 7

Conclusion

The highest increase in the temperature due to climate change is likely to occur during the winter season in Trøndelag. This could lead to change in the flood pattern in Ilabekken, as the large combination floods in the spring could decrease as a result of lower snow melt. Climate projections indicate that floods during the autumn season will most likely occur more often and at a larger scale in the future due to more precipitation.

The 200 year flood event is computed to be 17.14 m^3/s. This magnitude is based on a 6 hours synthetic storm event computed by statistical precipitation data from Voll observation site. The simulation shows that Theisendammen will have a damped effect on the runoff. Since there are three larges lakes in the catchment, these will likely have a reducing effect and contribute to a delay of the runoff. To include the changes in the future due to a changing climate the design flood is set to be Q_{200} with an increase of 20 %, which gives a magnitude of 20.59 m^3/s. The simulations in HEC-RAS shows that the flood magnitudes will contribute to variations in the flow pattern along the stream. The occurrence of hydraulic jumps in the stream indicates release of energy, which can contribute to erosion downstream. During 200 year flood event it will likely be flooding in the lowest part of the modelled reach. It has been estimated that the capacity of the culvert under Reservedammen will not be exceed during a flood event of 24.00 m^3/s.

The main trend in the computations of D_{50} indicate that increasing runoff will induce larger stable stone sizes, however this is not the case in all part of the stream. In shallow areas the size of D_{50} will decrease with increasing runoff due to higher water depths and decreasing velocity. The computations of D_{50} give an indication of the size a stone needs to be to be stable in a part of the stream. The computation of stable stone size, shows that the HEC-11 method

is very sensitive when the angle of the side slope approach the angle of repose. This method should be used carefully when estimating stable stone sizes in steep side slopes.

Transport of sediments can lead to sedimentation in the lower parts of the stream where the velocity decreases due to more shallow areas. It has already been observed in the reopening part. A consequence is poorer biological diversity in the area, due to accumulation of sediments and mud.

7.1 Future Work

As shown in the sensitivity analysis of the calibrated parameters in the HEC-HMS model, the constant loss rate and the base flow are estimated to be the most sensitive parameters. To obtain a higher correlation between the simulated runoff and the observed runoff at Kobberdammen, these parameters could be further investigated. To be able to estimate the constant loss rate more precisely it will be of interest to investigate the soil types in the catchment in more detail. As the model is sensitive to the base flow, this value should be more studied to obtain a better model result.

The sensitivity analysis of the roughness coefficients in the HEC-RAS model shows that the water level are sensitive to change in the n-values. To improve the quality and accuracy of the HEC-RAS model, a calibration of model could be conducted. To be able to say more about the possible consequences in the lower part of the stream, it could be beneficial to continue the HEC-RAS model further down the stream. This was originally planned to do in this thesis. Since the area downstream from the modelled part contains steep side slopes and lots of vegetation, it has been challenging to survey the cross sections in this part. In further work, the cross sections should be measured by using other equipments than GPS measurement as the area has poorly reception of GPS signals. It is not the most optimal time of the year to perform field measurements in the autumn, winter and early spring as done in this thesis due to ice and snow in the stream area. An idea is to conduct the measurements during the summer when ice and snow are not a problem. A continuing of the HEC-RAS model could make the evaluation of the risk of erosion and flooding in the reopened part more accurate. To be able to say something about the amount of sediment transport in the river, a sedimentation simulation in HEC-RAS can be conducted. This type of simulation requires geological information, such as types of sediments and grain size distribution in the area.

Bibliography

Ackerman, C. (2009). Hec-georas–gis tools for support of hec-ras using arcgis, user's manual. *US Army Corps of Engineers–Hydrologic Engineering Centre: Davis, CA*.

Barker, T., Davidson, O., Davidson, W., Huq, S., Karoly, D., Kattsov, V., Liu, J., Lohmann, U., Manning, M., Matsuno, T., et al. (2007). Climate change 2007: Synthesis report. *Valencia; IPCC*.

Berenbrock, C., Rousseau, J. P., and Twining, B. V. (2007). *Hydraulic Characteristics of Bedrock Constrictions and an Evaluation of One-and Two-Dimensional Models of Flood Flow on the Big Lost River at the Idaho National Engineering and Environmental Laboratory, Idaho*. US Department of the Interior, US Geological Survey.

Bergan, M. (2010). Bunndyrovervåking i ilabekken, trondheim kommune. undersøkelser i 2009. *Norsk institutt for vannforskning*.

Brown, S. A. and Clyde, E. S. (1989). Design of riprap revetment.

Brunner, G. W. (2010). Hec-ras river analysis system. hydraulic reference manual. version 4.1.

Bulcock, H. and Jewitt, G. (2010). Hydrological modeling system, hec-hms user's manual. *Hydrology and Earth System Sciences*, 14(2):383–392.

Crowe, C. T., Elger, D. F., Williams, B. C., and Roberson, J. A. (2010). *Engineering Fluid Mechanics, SI Version*, volume 9. John Wiley Sons, Inc.

Cunderlik, J. and Simonovic, S. (2004). Calibration, verification, and sensitivity analysis of the hec-hms hydrologic model, cfcas project: Assessment of water resources risk and vulnerability to changing climatic conditions. *Project report IV*.

Direktoratet for byggkvalitet (2010). Byggeteknknisk forskrift med veiledning (TEK10), § 7-2. Sikkerhet mot flom og stormflo.

Feldman, A. D. (2000). *Hydrologic modeling system HEC-HMS: technical reference manual*. US Army Corps of Engineers, Hydrologic Engineering Center.

Fergus, T., Hoseth, K., and Sæterbø, E. (2010). Vassdragshåndboka: håndbok i vassdragsteknikk. *Ny rev. utg. Trondheim: Tapir akademisk forl.*

Finans Norge (2015). Mye flomskader i 2014. URL: https://www.fno.no/aktuelt/nyheter/2015/01/mye-flomskader-i-2014. [Visited 19.04.2015].

Gilli, É., Mangan, C., and Mudry, J. (2012). *Hydrogeology: Objectives, Methods, Applications*. CRC Press.

Hanssen-Bauer, I., Drange, H., Førland, E. J., Roald, L. A., Børsheim, K. Y., Hisdal, H., Lawrence, D., Nesje, A., Sandven, S., Sorteberg, A., et al. (2009). Klima i norge 2100. bakgrunnsmateriale til nou klimatilpasning.

IPCC (2014). Climate change 2014 synthesis report.

Jenssen, L. and Tesaker, E. (2009). Veileder for dimensjonering av erosjonssikring av stein. *NVE*.

Lawrence, D. and Hisdal, H. (2011). Hydrological projections for floods in norway under a future climate. *NVE, Oslo*.

Nakicenovic, N. and Swart, R. (2000). Special report on emissions scenarios. *Special Report on Emissions Scenarios, Edited by Nebojsa Nakicenovic and Robert Swart, pp. 612. ISBN 0521804930. Cambridge, UK: Cambridge University Press, July 2000.*, 1.

Nøst, T. (2014). Vannovervåking i trondheim 2013. *Trondheim kommune*.

Ødegaard, H. (2012). *Vann-og avløpsteknikk*. Norsk Vann.

Rinde, T. (2014). Lecture 12 - HEC-RAS. TVM4106 Hydrological Modelling, autumn 2014.

Te Chow, V. (1959). *Open channel hydraulics*. McGraw-Hill Book Company, Inc; New York.

Appendices

1. Thesis Description

Master thesis spring 2015

Subject area : Hydrology, modelling and urban streams
Title: *Hydrological Modelling of the Ilabekken Catchment, and Flood Simulations of Ilabekken using HEC-HMS and HEC-RAS*

Ilabekken is an urban stream with an upper portion of natural stream segments and more urban elements towards the downstream end. The stream is known for high flows during heavy precipitation events and in combination of precipitation and snowmelt. The outlet from the stream's head water, the Theisendammen lake is a broad crested overflow dam. There is also a low flow valve regulating and ensuring minimum flow during low flow or drought. This thesis will build upon the project work from last fall (2014), where a literature study and field work surveying cross sections of the upper portion of the stream were conducted. A hydrological model of the catchment upstream from Ilabekken will be created. The upper part of Ilabekken will be modelled in HEC-RAS to evaluate climate change impact on flood and erosion protection measures.
Deliverables will be:

- Calibrated HEC-HMS model of the catchment upstream of Ilabekken
- HEC-RAS model of the upper part of Ilabekken
- Climate change scenarios evaluating the present and future erosion and flood risk in the stream
- Evaluation of erosion protection measures in the upper portion of the stream

Partner(s): Trondheim Kommune
Place of work: The master thesis will be conducted at the Department of Hydraulic and Environmental Engineering in Trondheim
Advisor(s): Tone M. Muthanna

2. HEC-HMS

This appendix contains some input data to HEC-HMS and tables of the sensitive parameters which was not included in the main report. The electronic part of this appendix includes the calibration model and the simulation model of Q_{200}.

Table 1 gives the input data used for model the reservoirs in the catchment. The rating curve of the discharge from the V-notch at Kobberdammen is computed by using the equation 2.2 presented in 2.3.

	Kobberdammen	Baklidammen	Theisendammen
Surface area $[m^2]$	70 000	83 000	83 000
Elevation [m.a.s.l.]	288	196	153
Initial condition	Elevation: 287 m	Inflow = outflow	Inflow = outflow
Outflow structure	Spillway: Specified (V-notch) Rating curve No. of spillways: 1 Dam top: Level overflow Elevation: 290 m Length: 70 m Discharge coefficient: 1.5	Spillway: Ogee weir No. of spillways: 2 Approach depth:2 m Approach loss: 0 Crest elevation: 196 m Crest length: 5 m Apron elevation: 194 m Apron length: 5 m Design head: 1 m	Spillway: Broad-crested weir No. of spillways: 1 Elevation: 153 m Length: 10 m Discharge coefficient: 1.4

Table 1: Initial conditions and input data of the reservoirs in the HEC-HMS model.

Sensitivity Analysis

The parameters effecting the model result in addition to the initial loss rate and the base flow are given in the tables 2, 3 and 4.

	Parameter change [%]	Max canopy storage[m^3/s]	Simulated peak flow [m^3/s]	Peak flow change [%]
Summer 2011	10	3.74	0.209	0.95
	0	3.40	0.211	0.00
	-10	3.06	0.213	0.95
Summer 2012	10	3.74	0.148	0.00
	0	3.40	0.148	0.00
	-10	3.06	0.148	0.00
Summer 2013	10	3.74	0.107	0.93
	0	3.40	0.108	0.00
	-10	3.06	0.108	0.00

Table 2: Sensitivity analysis of the maximum storage capacity

	Parameter change [%]	Time of Concentration [m^3/s]	Simulated peak flow [m^3/s]	Peak flow change [%]
Summer 2011	10	3.74	0.21	0.47
	0	3.40	0.211	0.00
	-10	3.06	0.211	0.00
Summer 2012	10	3.74	0.147	0.68
	0	3.40	0.148	0.00
	-10	3.06	0.148	0.00
Summer 2013	10	3.74	0.108	0.00
	0	3.40	0.108	0.00
	-10	3.06	0.108	0.00

Table 3: Sensitivity analysis of the time of concentration

	Parameter change [%]	Storage Coefficient [m^3/s]	Simulated peak flow [m^3/s]	Peak flow change [%]
Summer 2011	10	1.65	0.209	0.95
	0	1.50	0.211	0.00
	-10	1.35	0.212	0.47
Summer 2012	10	1.65	0.147	0.68
	0	1.50	0.148	0.00
	-10	1.35	0.148	0.00
	10	1.65	0.107	0.93
	0	1.5	0.108	0.00
	-10	1.35	0.108	0.00

Table 4: Sensitivity analysis of the storage coefficient

3. HEC-RAS

This appendix includes an overview of the cross sections and output plots from the simulations in the HEC-RAS model. The electronic part of this appendix includes the HEC-RAS model and the measured coordinates of the river geometry. An overview of the cross sections used in the establishment of the model are shown in figure 1.

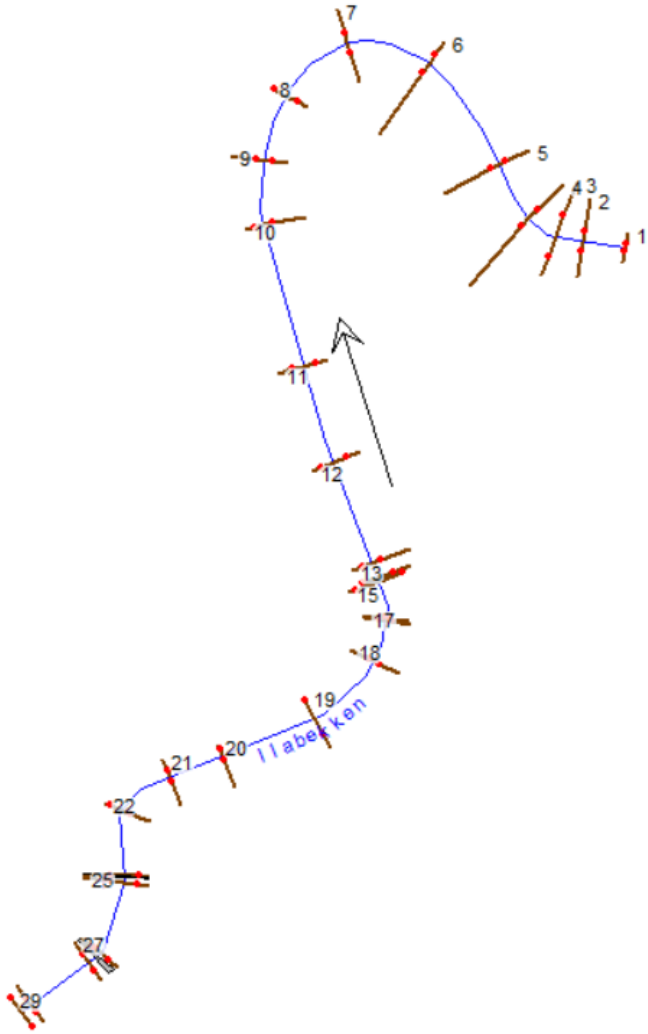

Figure 1: Overview of the cross sections

Figure 2 and figure 3 show the longitudinal profile plot of the modelled reach during the flood event of Q_{200} and $Q_{200+40\%}$.

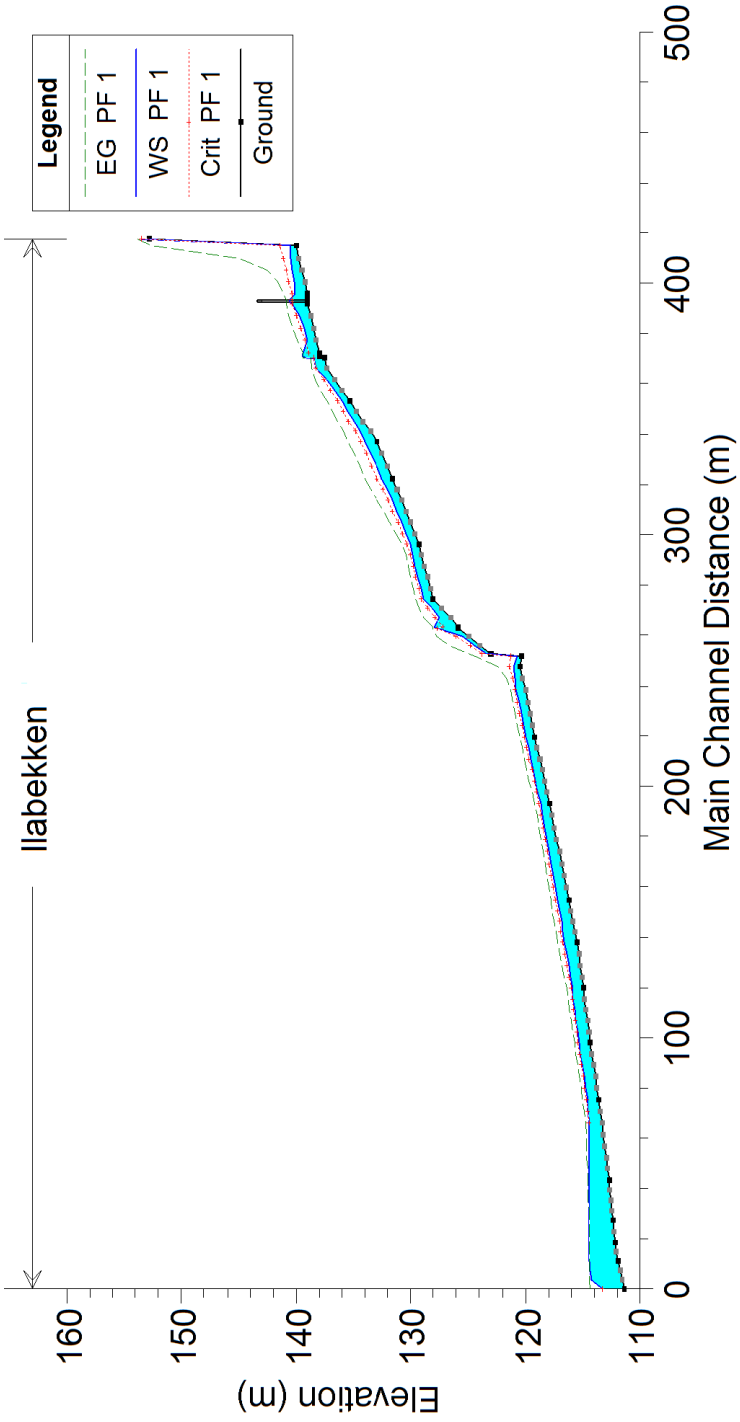

Figure 2: Longitudinal profile plot of Q_{200}

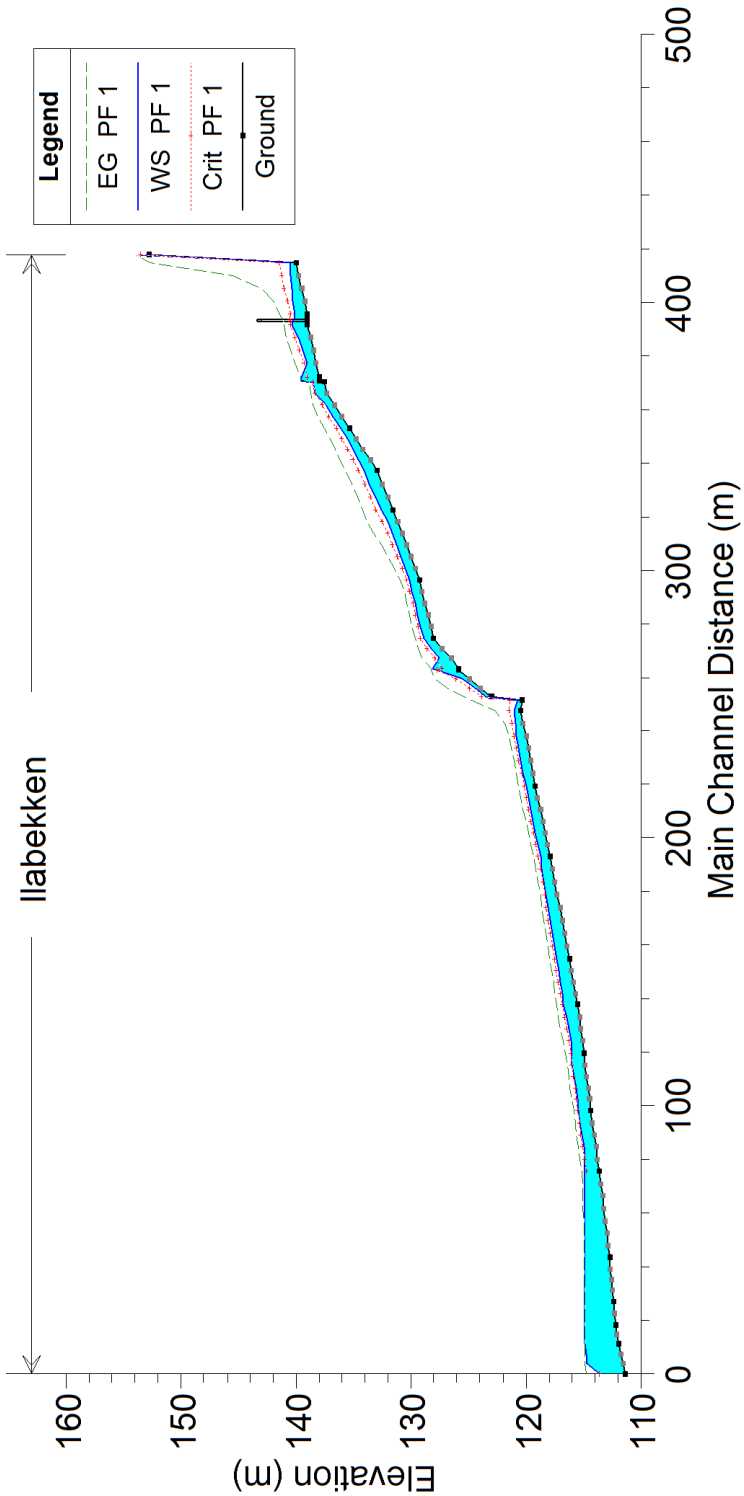

Figure 3: Longitudinal profile plot of $Q_{200+40\%}$

Figure 4, 5 and 6 show the water stage elevation at the inlet of the culvert during each of the flood scenarios.

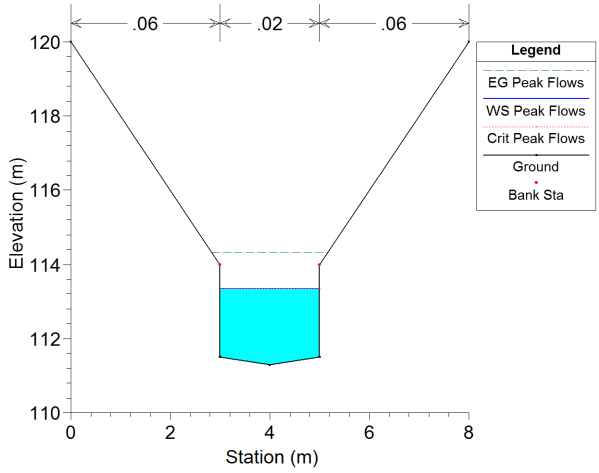

Figure 4: The water stage elevation at the inlet of culvert during Q_{200}

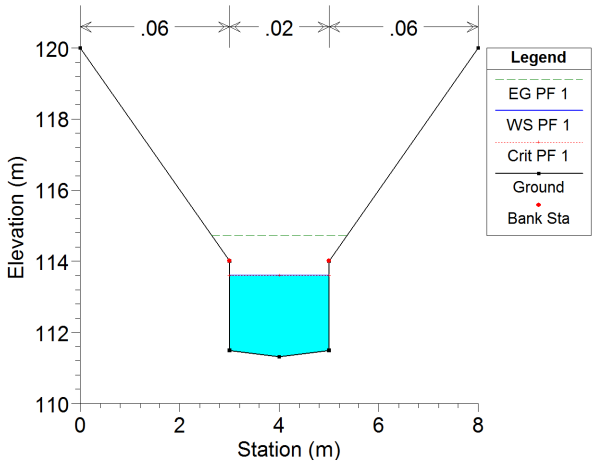

Figure 5: The water stage elevation at the inlet of culvert during $Q_{200+20\%}$

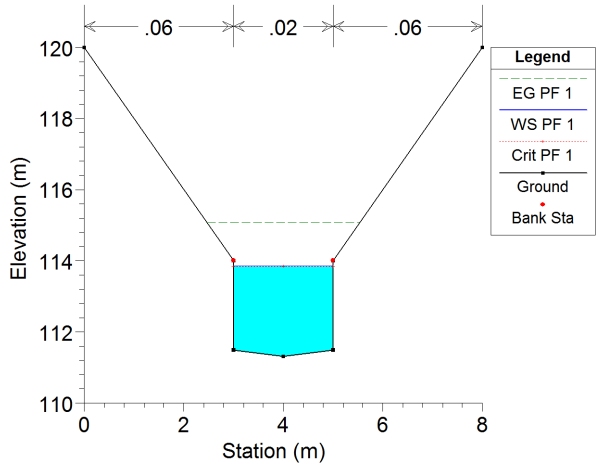

Figure 6: The water stage elevation at the inlet of culvert during $Q_{200+40\%}$

4. Input to the Compution of Stable Stone Size

This appendix provides the input data required in the computation of the stable stone size in the evaluated cross sections. Table 5 shows general information of the cross sections. Table 6 shows the input data required in the Shields equation. The correction factors are given in tables in the NVE report 4-2009 [Jenssen and Tesaker, 2009]. Table 7 shows the input data required in the HEC-11 method. The selected angle of repose used in the computations, is based on information found in the NVE report 4-2009.

Parameter	22	18	12	10	8.75*	8	7	6.6*	6.2*
Curve radius [m]	20.0	20	100.0	95.0	50.0	50.0	25.0	45.0	45.0
Width (average) [m]	8.7	10.8	9.4	13.0	8.7	9.1	13.4	13.1	17.4
Curve ratio, R/W [-]	2.3	1.9	10.6	7.3	5.7	5.5	1.9	3.4	2.6
Delta h [m]	1.4	1.6	2.2	1.7	0.73	0.8	0.9	0.73	0.61
Delta l [m]	2	1.8	2.5	2.4	1.7	1.2	6.5	1.66	1.1
Side slope, n [-]	1.4	1.1	1.1	1.4	2.3	1.5	7.2	2.3	1.9
Specific stone density $[kg/m^3]$	2600	2600	2600	2600	2600	2600	2600	2600	2600

Table 5: General information of the cross sections evaluated

Parameter	22	18	12	10	8.75*	8	7	6.6*	6.2*
Shear stress channel, $[N/m^2]$	733.2	440.6	346.9	325.5	376.7	330.9	282.2	261.53	274.3
Correction for curve, [-]	2	2	1	1.3	1.48	1.49	2	1.8	1.83
Correction for side slope, [-]	1.75	2	2	1.75	1.13	1.3	1	1.13	1.2
Stability factor [-]	1.1	1.1	1.1	1.1	1.1	1.1	1.1	1.1	1.1

Table 6: Input data to Shields equation for the cross sections evaluated

Parameter	22	18	12	10	8.75*	8	7	6.6*	6.2*
Average velocity, V_{ch} [m/s]	5.57	4.59	3.59	3.64	3.89	3.56	3.31	3.2	3.26
Average depth, V_{ch} [m]	0.77	0.93	0.79	1.12	1.12	1.05	0.97	1.03	1.04
Stability factor, SF [-]	2	2	1.4	2	2	2	2	2	2
Angle of side slope, [°]	35	41.6	41.3	35.3	22.4	33.7	7.9	16.8	28.3
Angle of repose, ϕ [°]	42	42	42	42	42	42	42	42	42

Table 7: Input data to HEC-11 methodfor the cross sections evaluated

Plots of each of the evaluated cross sections are presented below. The plots show the water stage elevation during the design flood.

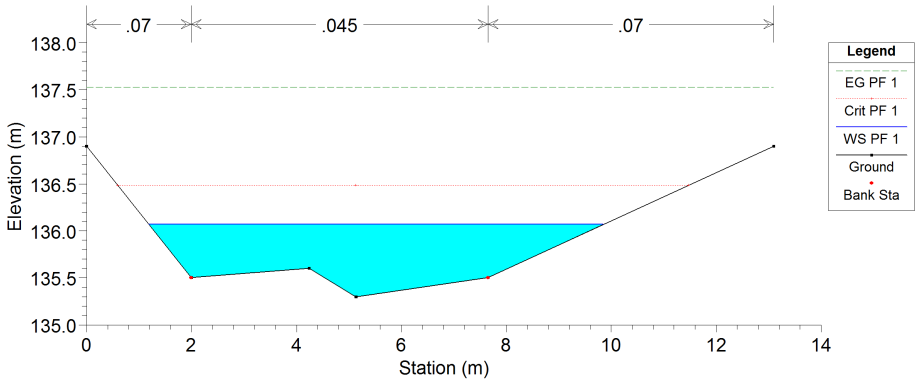

Figure 7: Cross section 22

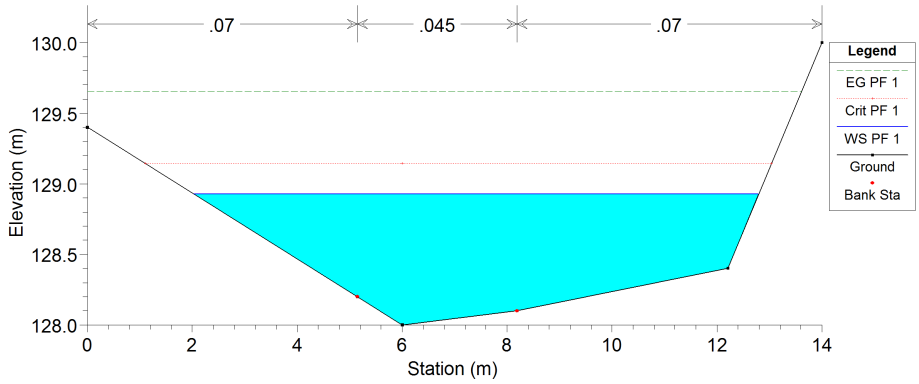

Figure 8: Cross section 18

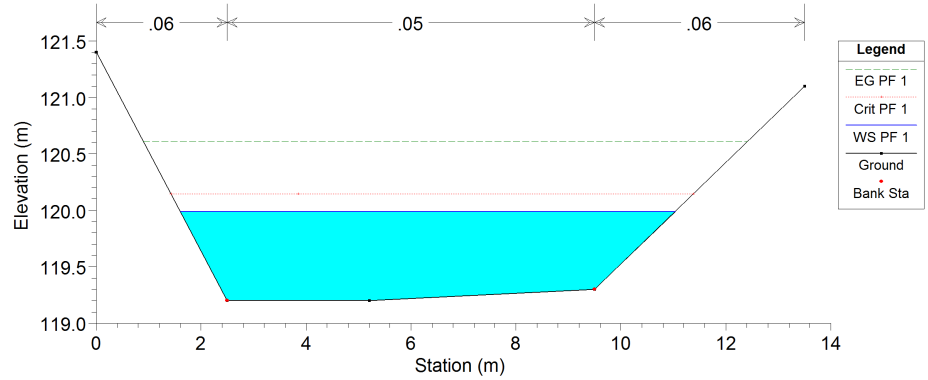

Figure 9: Cross section 12

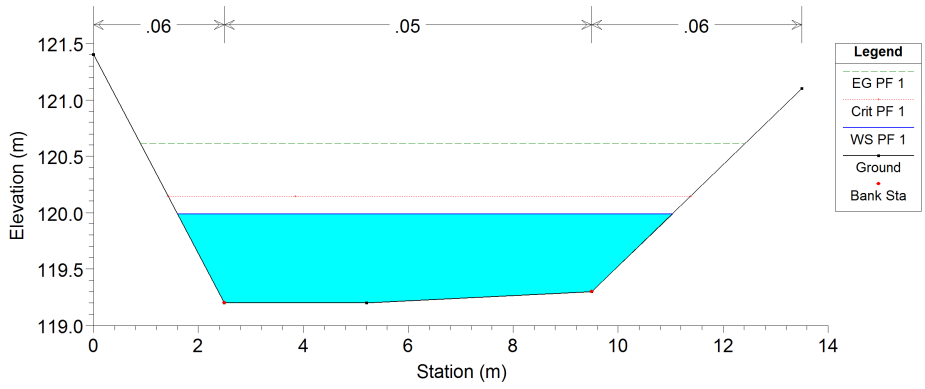

Figure 10: Cross section 10

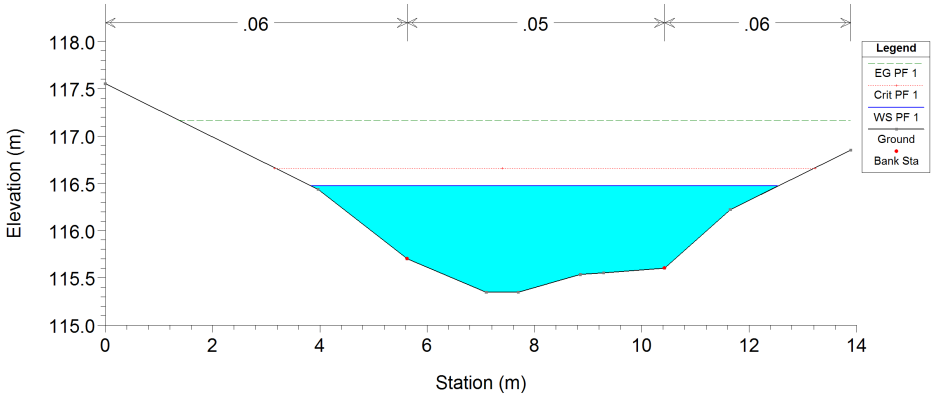

Figure 11: Cross section 8.75*

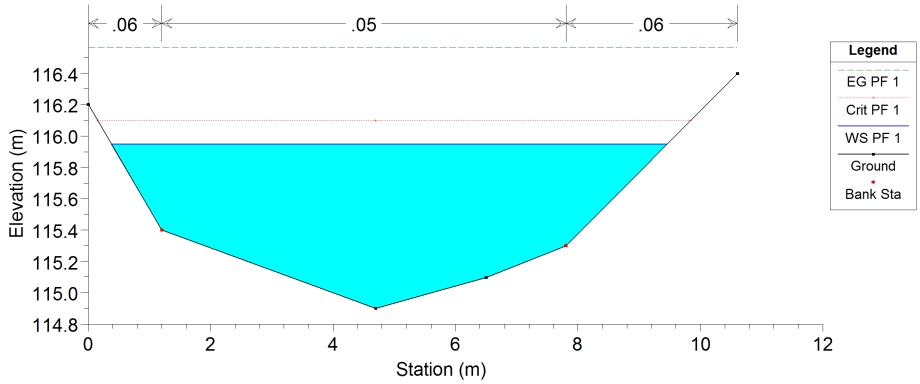

Figure 12: Cross section 8

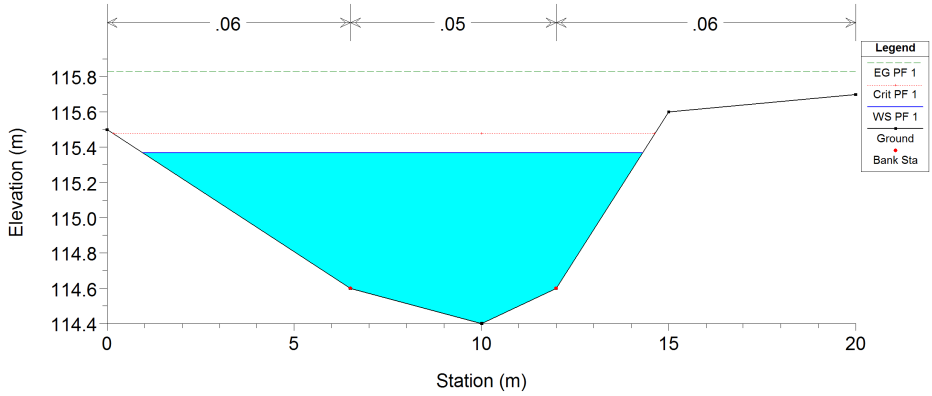

Figure 13: Cross section 7

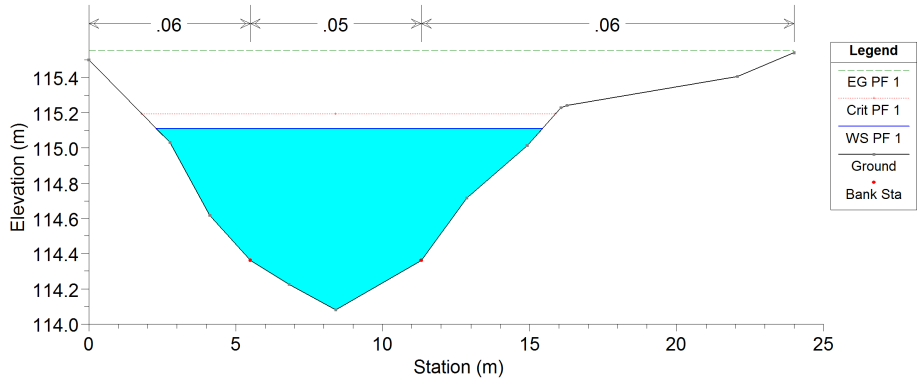

Figure 14: Cross section 6.6*

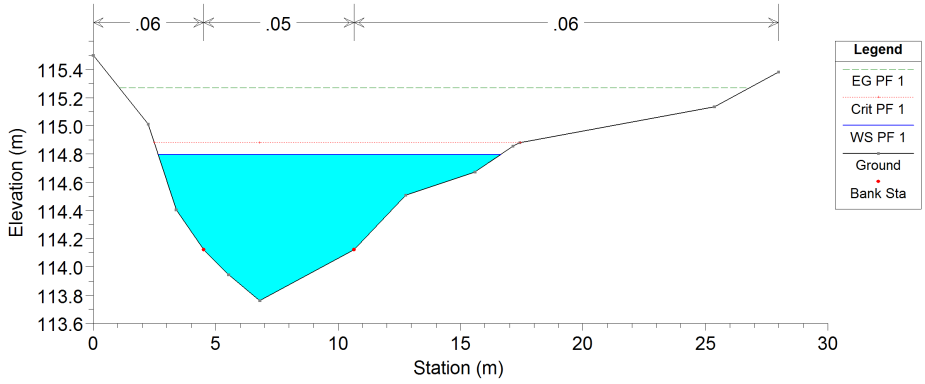

Figure 15: Cross section 6.2*

The picture in figure 16 shows observed erosion at the cross section 12. This picture was taken during the field work.

Figure 16: Observation of erosion at cross section 12